International Journal of Pharmaceutics 452 (2013) 135–156

Contents lists available at SciVerse ScienceDirect

International Journal of Pharmaceutics

journal homepage: www.elsevier.com/locate/ijpharm

Preparation and evaluation of agglomerated crystals by crystallo-co-agglomeration: An integrated approach of principal component analysis and Box–Behnken experimental design

Kevin C. Garala[a,*], Jaydeep M. Patel[a], Anjali P. Dhingani[a], Abhay T. Dharamsi[b]

[a] Department of Pharmaceutics, Atmiya Institute of Pharmacy, Rajkot 360005, India
[b] Department of Pharmaceutics, Maliba Pharmacy College, Surat, 394350, India

ARTICLE INFO

Article history:
Received 1 March 2013
Received in revised form 25 April 2013
Accepted 25 April 2013
Available online 14 May 2013

Keywords:
Principal component analysis
Box–Behnken design
Agglomerative hierarchy cluster analysis
Crystallo-co-agglomeration
Racecadotril

ABSTRACT

Poor mechanical properties of crystalline drug particles require wet granulation technique for tablet production which is uneconomical, laborious, and tedious. The present investigation was aimed to improve flow and mechanical properties of racecadotril (RCD), a poorly water soluble antidiarrheal agent, by a crystallo-co-agglomeration (CCA) technique. The influence of various excipients and processing conditions on formation of directly compressible agglomerates of RCD was evaluated. Principal component analysis and Box–Behnken experimental design was implemented to optimize the agglomerates with good micromeritics and mechanical properties.

The overall yield of the process was 88–98% with size of agglomerates between 351 and 1214 μm. Further, higher rotational speed reduced the size of agglomerates and disturbed sphericity. The optimized batch of agglomerates exhibited excellent flowability and crushing strength.

The optimized batch of RCD agglomerates was characterized by fourier transform infrared spectroscopy, differential scanning calorimetry, powder X-ray diffractometry and gas chromatography which illustrated absence of drug–excipient interaction with minimal entrapment of residual solvent. Hence, it may be concluded that both excipients and processing conditions played a vital role to prepare spherical crystal agglomerates of RCD by CCA and it can be adopted as an excellent alternative to wet granulation.

1. Introduction

Many active pharmaceutical ingredients are crystalline in nature with different crystal habits. These crystal habits play an important role in flowability, compactability, compression characteristics, packing, and dissolution (Rasenack and Müller, 2002a; Tiwari, 2001). For drugs with inadequate mechanical properties, wet granulation with or without excipients is the best option. However, wet granulation is a tedious technique with many disadvantages like high labor, uneconomical and time consuming (Joshi et al., 2003). Today, direct compression method for tableting is a prime choice by pharmaceutical industries to overcome the disadvantages. Nevertheless, direct compression is highly influenced by the physical properties of drug (Usha et al., 2008; Paradkar et al., 2010).

Drugs with poor compressibility and flowability are unsuitable for direct compression. Particle size enlargement techniques employed in the field of pharmacy to improve flowability of compression blend include extrusion–spheronization (Gokonda et al., 1994), melt solidification (Paradkar et al., 2003), melt granulation (Johansen et al., 1999), melt extrusion (Sprockel et al., 1997), and spherical crystallization (SC) (Kawashima et al., 1982a,b). Among all, SC technique is superior in modifying crystal nature and produces directly compressible agglomerates. In addition to modifications in the primary and secondary properties of the particles, this technique also offers advantages in terms of reduction in the number of unit operations and thus, processing cost. The suitability of this technique relies on the desired properties of the enlarged particles and the physico-chemical properties of the drug and excipients used. The unsuitability of SC technique for low-dose and combination of drugs, Kadam et al. (1997) successfully overcame by

Abbreviations: AHCA, agglomerative hierarchy cluster analysis; CCA, crystallo-co-agglomeration; CCD, charged-coupled device; DCM, dichloro methane; DSC, differential scanning calorimetry; GC, gas chromatography; HPLC, high performance liquid chromatography; HPMC, Hydroxypropyl methylcellulose; ICH, international conference on harmonization; PCA, principal component analysis; PEG, polyethylene glycol; PVA, polyvinyl alcohol; PXRD, powder X-ray diffraction; rpm, revolution per minute.

* Corresponding author at: Atmiya Institute of Pharmacy, Yogidham Gurukul, Kalawad Road, Rajkot 360005, India. Tel.: +919974664666; fax: +91 281 2563766.
E-mail addresses: kevincgarala@gmail.com (K.C. Garala), jmpatel7@gmail.com (J.M. Patel), anjali.patel27@gmail.com (A.P. Dhingani), aadharamsi@gmail.com (A.T. Dharamsi).

0378-5173/$ – see front matter © 2013 Elsevier B.V. All rights reserved.
http://dx.doi.org/10.1016/j.ijpharm.2013.04.073

adopting crystallo-co-agglomeration (CCA) technique. CCA, a novel particle engineering technique, is a modification of SC in which a drug is crystallized and agglomerated with excipient(s) or with another drug, which may or may not be crystallized in the system.

In CCA, crystals of drug aggregate in the form of small spherical particles along with excipients and solvents were used to develop an intermediate material with improved micromeritic and mechanical properties (Pawar et al., 2004a). The rate of dissolution of drug from the agglomerates or compacts thereof were improved and modified by using suitable excipients during the process of agglomeration (Maghsoodi et al., 2008; Jadhav et al., 2007). Various studies have already been reported for the drugs with low aqueous solubility, poor physico-chemical and physico-mechanical properties. This includes ibuprofen (Pawar et al., 2004a), combination of ibuprofen with paracetamol (Pawar et al., 2004b), ketoprofen (Chavda and Maheshwari, 2008), naproxen (Maghsoodi et al., 2008), bromhexidine hydrochloride (Jadhav et al., 2010), aceclofenac (Sarfaraz et al., 2011), olmesartan medoxomil (Yadav et al., 2012), and secnidazole (Raval et al., 2013).

The present research work was aimed to develop agglomerates of RCD by CCA technique. The long needle like crystalline properties of RCD produce poor flowability and compressibility which ultimately cause difficulty in direct compression (Schwartz and Lecomte, 2009). Further, RCD is insoluble in water and this makes a rapid release of molecule by disintegration of the tablet more difficult (Schwartz and Lecomte, 2009). Hence, the authors endeavor to study the influence of processing conditions and effect of various excipients on the formation of agglomerates of RCD and its mechanical properties in order to obtain excellent flowability and compressibility for direct compression. To optimize agglomerates, principal component analysis (PCA), agglomerative hierarchy cluster analysis (AHCA), and Box–Behnken experimental design were employed in the study.

2. Materials and methods

2.1. Materials

RCD was procured from Ogene Systems (I) Pvt. Ltd., Hyderabad, India. Talc, PEG 6000 and PVA were purchased from HiMedia Labs, Mumbai, India. HPMC was gifted by Colorcon Asia Pvt. Ltd., Goa, India. High performance liquid chromatography (HPLC) grade acetonitrile and water were purchased from Merck Pvt. Ltd., Mumbai, India. All other chemicals used were of analytical grade (Merck Pvt. Ltd., Mumbai, India) and double distilled water was utilized throughout the study.

2.2. Preparation of crystal agglomerates

2.2.1. Selection of solvent system

Various solvents were screened with different polarity for selection of good solvent and poor solvent. An excess amount of RCD was added to each of selected solvents (5 mL) and all these saturated solutions were kept for 24 h in a cryostatic constant temperature (25 ± 1 °C) reciprocating shaker bath (Tempo Instruments and Equipments Pvt. Ltd., Mumbai, India) with constant stirring at 120 rpm (Batt and Garala, 2012; Raval et al., 2013). The concentration of drug in each solvent was then determined by HPLC (Shimadzu, Japan) and the study was repeated thrice to estimate reproducibility of results.

2.2.2. Selection of excipients and processing conditions

Various excipients (Talc, Polyvinyl pyrrolidone K30 (PVP), Hydroxy propyl cellulose (HPC), Ethyl cellulose (EC), Hydroxy propyl methyl cellulose E50LV (HPMC), Polyvinyl alcohol (PVA), Polyethylene glycol 6000 (PEG) and Eudragit S 100 (ERS)) were dissolved in a suitable medium in the different concentrations to study their influence on crystal-co-agglomerates of RCD. For optimization of types and concentrations of polymers, various preliminary trials were performed. Other parameters like stirring speed, temperature and phase ratio were kept constant during the excipients selection study. The selection criteria were based on mean geometric diameter (dg), angle of repose (AoR) and crushing strength (CS). An optimized batch of agglomerates with selected excipients was subjected to various stirring speeds (200–1200 rpm) using a propeller type of agitator at room temperature and was analyzed by a dg, AoR and CS. Further, to study the effect of temperature, the previously optimized batch of agglomerates was prepared at various temperature conditions and evaluated by a dg, AoR and CS. In addition, to determine the effect of the phase ratio on agglomeration, different ratios of good solvent and poor solvent were employed and the agglomerates obtained were evaluated by various parameters like dg, AoR and CS.

Table 1
Box–Behnken design batches.

Batch code	Independent variables		
	X_1 [a]	X_2 [b]	X_3 [c]
R1	−1	−1	0
R2	1	−1	0
R3	−1	1	0
R4	1	1	0
R5	−1	0	−1
R6	1	0	−1
R7	−1	0	1
R8	1	0	1
R9	0	−1	−1
R10	0	1	−1
R11	0	−1	1
R12	0	1	1
R13	0	0	0

Factor	Level		
	−1	0	1
X_1 (DCM: water)	0.04	0.07	1
X_2 (Concentration of PEG 6000, %w/w)	2	3.5	5
X_3 (Speed, rpm)	600	800	1000

2.2.3. Crystallization procedure

On the basis of solubility study, good solvent and poor solvent was identified for the preparation of agglomerates by CCA technique. In crystallization vessel, as described by Morishima et al. (1993), RCD (1 gm) was dissolved in good solvent followed by talc (1% w/w) and PVA (1.5% w/w). To 100 mL of poor solvent, 1%w/w HPMC E50 LV and PEG 6000 (Table 1) was added in a crystallization vessel and these contents were stirred at specific speed by using four blade mechanical stirrer. The stirring was continued until the mixture appeared clear at top along with settling of agglomerates. The agglomerates generated were filtered and dried overnight at room temperature. The dried agglomerates were stored in screw-capped jars at room temperature before evaluation. The effect of different concentrations of excipients was investigated and optimized (Raval et al., 2013).

2.3. Box–Behnken experimental design

Box–Behnken statistical screening design was employed to evaluate main effects and interaction effects of independent variables on the various properties of RCD agglomerates in order to optimize the formulation. The non-linear quadratic model generated by the

design is as follows:

$$Y_i = b_0 + b_1X_1 + b_2X_2 + b_3X_3 + b_{12}X_1X_2 + b_{23}X_2X_3 + b_{13}X_1X_3 + b_{11}X_1^2 + b_{22}X_2^2 + b_{33}X_3^2 \quad (1)$$

where, Y_i is dependent variable, b_0 is arithmetic mean response of 13 runs and b_i is the estimated coefficient for factor X_i. The main effects (X_1, X_2 and X_3) signify average result of altering one factor at a time from its lowest to highest value. The interaction terms (X_1X_2, X_2X_3 and X_1X_3) prompt change in responses when two factors are simultaneously altered. The polynomial terms (X_1^2, X_2^2 and X_3^2) are added to investigate non-linearity of the model (Maurya et al., 2011). A three-factor, three-level Box–Behnken design was generated by an experimental design software SYSTAT version 12.02.00 (SYSTAT Software Inc., Chicago, USA). Based on preliminary trials, independent variables (factors) were determined as: ratio of good solvent (dichloromethane, DCM) to poor solvent (water) (X_1), concentration of PEG 6000 (X_2) and stirring speed (X_3). The formulation composition is summarized in Table 1.

Additionally the composition of optimized (check point) batch was derived by constructing overlay plot. The percentage relative error of each response was calculated using following equation in order to judge validity of the model (Singh et al., 2005a, b; Shah et al., 2007).

$$\%\text{Relative Error} = \frac{|\text{Predicted value} - \text{Experimental value}|}{\text{Predicted value}} \times 100 \quad (2)$$

2.4. Drug loading efficiency and percent yield

Drug loading efficiency is the ratio of experimentally measured drug content to the theoretical value, expressed as percentage (%). Accurately weighed quantity of prepared agglomerates was dissolved in sufficient quantity of a suitable solvent in which they were easily soluble. These solutions were appropriately diluted and drug content was determined by previously validated HPLC method (Kevin et al., 2012). The percent (%) yield of samples was calculated using following equation (Chaulang et al., 2008). Average of three determinations was considered as mean value for both parameters.

$$\%\,\text{Yield} = \frac{\text{Total weight of agglomerates}}{\text{Total weight of drug and excipients}} \times 100 \quad (3)$$

2.5. Size analysis

The size of pure drug particles and prepared agglomerates was measured by optical microscope (MLX-DX, Olympus (I) Pvt. Ltd., New Delhi, India). The size of randomly selected particles or agglomerates was measured and their mean geometric diameter (dg) was calculated (Martin et al., 1991).

2.6. Shape analysis

Shape parameters of pristine RCD and prepared agglomerates were evaluated based on the projected images of randomly positioned particles. The photomicrographs of the randomly selected agglomerates were taken using CCD camera (MIPS-USB, Olympus (I) Pvt. Ltd., New Delhi, India) and tracings of the enlarged photomicrographs were used for the measurement of length, width, area and perimeter. Numerous shape descriptors like aspect ratio (AR), shape factor (SF), circularity factor (CF) and irregularity factor (IF) were evaluated as per equation (4)–(7), respectively. Results of each parameters recorded was the average of three determinations.

$$\text{AR} = b/l \quad (4)$$

where b and l are minor and major axis of traced photograph, respectively.

$$\text{SF} = P'/P \quad (5)$$

where $P' = 2\pi(\text{A}/\pi)^{1/2}$, A and P is area and perimeter of the projected photograph, respectively.

$$F = (P')^2/4\pi A \quad (6)$$

$$IF = P/l \quad (7)$$

2.7. Flow parameters

AoR was determined using fixed funnel method (Pilpel, 1964). Percentage compressibility (Carr's Index, CI) (Carr, 1965) and Hausner's ratio (HR) (Hausner, 1967) was calculated after tapping fixed amount of agglomerates using tap density apparatus (ETD 1020, Electrolab, Mumbai, India). Average of three determinations was considered as final results.

2.8. Measurement of packability

2.8.1. Kawakita analysis

The packing ability of coarse RCD and prepared agglomerates was investigated by tapping them into a measuring cylinder using a tap density apparatus (ETD 1020, Electrolab, Mumbai, India). The packability was calculated by the following equation (Kawakita and Tsutsumi, 1966).

$$\frac{n}{c} = \frac{1}{ab} + \frac{n}{a} \quad (8)$$

where, a and b are constants, n is tap number, C denotes volume reduction and calculated using the following equation:

$$C = \frac{V_O - V_n}{V_O} \quad (9)$$

where, V_O and V_n are the powder or agglomerate bed volumes at initial and nth tapped state, respectively. Average of three determinations was considered as mean of individual Kawakita parameters.

2.8.2. Kuno analysis

The relationship between the change in apparent density and the number of tappings was described by Kuno as per following equation (Kuno, 1979).

$$\ln(\rho_t - \rho_n) = -Kn + \ln(\rho_t - \rho_o) \quad (10)$$

where ρ_t is the apparent density at infinite taps, ρ_n is the apparent density at nth tapped state, ρ_o is the apparent density at initial cascade state and the constant K represents the rate of packing process under tapping (Mallick et al., 2011).

2.8.3. Heckel analysis

Accurately weighed quantity of pure drug and agglomerates were compressed by hydraulic press (TechnoSearch Instrument, Mumbai, India) at constant compression with different pressures and dwell time of 1 min (Jadhav et al., 2007). Before compression, lubrication of die and punches was carried out by 1% w/v dispersion of magnesium stearate in acetone. Compacts were allowed to relax

Table 2
Selection of excipients for RCD agglomeration.

Trial	Excipients	Concentration (%w/w)	Results[a]		
			dg (μm)	AoR (°)	CS (gm)
PR1	Talc	0	108.56 ± 9.37	38.55 ± 3.82	8.43 ± 1.04
PR2		0.5	194.51 ± 11.19	36.11 ± 2.93	18.34 ± 1.31
PR3		1.0	327.18 ± 17.21	30.65 ± 1.57	25.51 ± 2.02
PR4		1.5	275.15 ± 20.52	32.61 ± 2.94	15.91 ± 2.28
PR5		2.0	211.36 ± 18.68	35.96 ± 3.07	13.89 ± 1.87
PR6	PVP	0.5	228.47 ± 15.21	30.52 ± 1.04	21.72 ± 1.96
PR7		1.0	247.28 ± 35.63	29.63 ± 2.52	19.37 ± 2.81
PR8		1.5	269.67 ± 27.81	31.54 ± 2.31	19.64 ± 2.57
PR9		2.0	253.82 ± 24.92	30.57 ± 1.84	21.55 ± 2.63
PR10	HPC	0.5	284.54 ± 20.62	29.75 ± 1.26	23.12 ± 1.58
PR11		1.0	249.72 ± 32.53	31.59 ± 2.59	20.53 ± 2.54
PR12		1.5	274.31 ± 25.58	30.07 ± 2.64	21.51 ± 1.85
PR13		2.0	268.79 ± 36.69	28.94 ± 2.28	22.45 ± 1.82
PR14	EC	0.5	183.62 ± 18.87	27.12 ± 2.92	34.52 ± 3.41
PR15		1.0	232.57 ± 22.61	28.64 ± 3.54	31.05 ± 1.96
PR16		1.5	224.06 ± 23.45	29.62 ± 3.29	32.46 ± 2.34
PR17		2.0	213.34 ± 22.58	30.05 ± 2.47	30.71 ± 2.17
PR18	HPMC	0.5	279.56 ± 28.63	28.46 ± 2.19	32.14 ± 3.55
PR19		1.0	342.62 ± 34.51	27.93 ± 2.12	36.82 ± 4.03
PR20		1.5	352.24 ± 38.29	26.41 ± 3.26	33.13 ± 3.58
PR21		2.0	349.54 ± 40.13	27.15 ± 2.17	34.26 ± 2.74
PR22	PVA	0.5	324.62 ± 59.36	28.45 ± 2.51	33.15 ± 1.53
PR23		1.0	351.49 ± 74.21	28.64 ± 3.08	30.54 ± 3.15
PR24		1.5	368.26 ± 31.27	27.39 ± 1.59	34.26 ± 2.18
PR25		2.0	354.23 ± 28.42	27.64 ± 2.56	28.32 ± 2.43
PR26	PEG	1.0	224.96 ± 21.14	29.31 ± 0.73	26.24 ± 1.49
PR27		2.0	637.63 ± 34.68	23.38 ± 2.11	34.85 ± 1.92
PR28		3.0	886.32 ± 38.72	22.23 ± 1.72	37.33 ± 2.66
PR29		4.0	1095.7 ± 103.5	22.64 ± 0.97	44.27 ± 3.08
PR30		5.0	1318.4 ± 147.3	27.52 ± 4.93	42.35 ± 4.32
PR31		6.0	2173.2 ± 455.6	35.13 ± 4.36	33.62 ± 3.11

[a] Results are mean of three observation ±SD.

for 24 h at ambient temperature and the data obtained was subjected to Heckel plot using the following equation (Heckel, 1961a, b).

$$\ln \frac{1}{1-D} = kPy + A \tag{11}$$

where D is relative density of compacts i.e. ratio of compact density to true density of powder, P is the applied compression pressure, and k and A are constants. The reported mean yield pressures, Py, are the reciprocal of the slope k, which was calculated using linear regression in a pressure range determined separately for each material. k is equal to $1/3\sigma_o$, where, σ_o is yield strength and $3\sigma_o$ as mean yield pressure (Py). Here, density of prepared compacts for Heckel parameter was calculated from volume of compacts and mass of compacts. Average of three determinations was considered as mean of respective Heckel parameters.

2.9. Tensile strength

The radial tensile strength (σ_t) of coarse RCD or agglomerates is considered as force per unit area of broken face required to split a prepared compact. The data used for compressional studies of prepared agglomerates were used to study the pressure tensile strength relationship. The hardness value of compacts was determined by a Monsanto type hardness tester and used for σ_t determination using the following equation (Fell and Newton, 1970). Average of three determinations was considered as σ_t.

$$\sigma_t = \frac{2F}{\pi Dt} \tag{12}$$

where F is the crushing force (N), D is the tablet diameter, and t is the compact thickness.

2.10. Elastic recovery

The compacts prepared, form coarse RCD and agglomerates, for the Heckel plot study and tensile strength determination were used for the elastic recovery test. The thickness of the compacts was measured immediately after ejection (Hc) and after 24 h relaxation period (He). The elastic recovery was calculated by the following equation (Armstrong and Haines-Nutt, 1974). Average of three determinations was considered as %ER.

$$\%\text{ER} = [(He - Hc)/Hc] \times 100 \tag{13}$$

2.11. Crushing strength

CS of prepared agglomerates was determined by mercury load cell method (Jarosz and Parrott, 1983). The agglomerate was placed inside the syringe and mercury was added through hollow syringe tube. The total weight of tube with mercury, at the stage where agglomerate broke, gave measure of CS of agglomerate. Average of three determinations was considered as CS.

2.12. Percent moisture content

Moisture content (MC) of prepared agglomerates was determined by IR moisture balance (Rajdhani, Mumbai, India). The agglomerates (5 gm) were placed in a heating pan and heated at a temperature of 105 °C for 4 h. The percent reduction in the weight of agglomerates due to moisture loss was directly displayed on the scale. Average of three determinations was considered as % MC.

2.13. Scanning electron microscopy

The shape and surface morphology of pure drug particles and prepared agglomerates were observed using scanning electron microscope (SEM) (JEOL, JSM 5610 LV, Japan). The agglomerates were observed at various magnifications in order to analyze the effect of additives on surface morphology and agglomeration efficiency.

2.14. Fourier transform-infrared (FT-IR) spectroscopy

Infrared spectra of pure drug and optimized agglomerates were recorded using infrared spectrophotometer (Nicolet iS10, Thermo Fisher Scientific Inc., USA). The samples were dispersed in KBr and compressed into disc by application of pressure using hydraulic press. The pellets were placed in the sample holder and FT-IR spectra were recorded over the range of 400–4000 cm^{-1}.

2.15. Differential scanning calorimeter (DSC) analysis

DSC spectra of pure drug, polymers and optimized agglomerates were recorded using differential scanning calorimeter (DSC-60, Shimadzu, Tokyo, Japan) which was previously calibrated with indium standard. Sample (~ 5–10 mg) was hermetically sealed in an aluminum crucible and subjected to purging of nitrogen gas at a flow rate of 50 mL/min. The heating was done at a rate of 10 °C/min. Empty sealed aluminum pan was used as reference (Srinivasan et al., 2011; Jun et al., 2012). The spectra obtained were analyzed for endothermic and exothermic transitions in drug agglomerates (Stodghill, 2010). The crystallinity (*Xcr*) was calculated as:

$$Xcr = \frac{\Delta H}{\Delta H_o} \quad (14)$$

where ΔH_0 and ΔH are the heat of fusion of the unprocessed and the treated crystals, respectively (Niwa et al., 2010).

2.16. Powder X-ray diffractometry (PXRD)

The X-ray powder diffraction patterns of pure drug particles and optimized agglomerates were recorded using diffractometer system (X'Pert MPD, Philips, Netherlands) with a copper target and scintillation counter detector (voltage 40 kV; current 30 mA; and scanning speed 0.05 °/s). The sample holder was non-rotating and temperature of acquisition was at room temperature. The diffraction pattern was analyzed for the 2θ range from 10° to 90° (Cooper et al., 2003).

2.17. Gas chromatography

Accurately weighed optimized agglomerates were suspended in methanol and shaken in orbital shaking incubator (Remi Laboratory Instruments, Mumbai, India) for 24 h at 100 rpm. Subsequently, the dispersion was filtered and filtrate was analyzed using gas chromatography (head space) GC-HS (Turbo matrix 40, PerkinElmer, USA) with column Rtx-5MS (thickness: 0.25 μm, diameter: 0.25 μm and length: 60 m) and Helium as carrier gas. The reference solution (1000 ppm) and sample solution were injected alternately to GC-HS and area of peak obtained was used to calculate the solvent concentrate in agglomerates.

2.18. In vitro dissolution study

In vitro dissolution study of pure drug and prepared agglomerates were performed using USP type II apparatus (TDT 06P, Electrolab, India) to evaluate the influence of various excipients on drug release from agglomerates. Acetate buffer pH 4.5 (900 mL) with 0.75% SLS was used as a dissolution medium and temperature was maintained at 37 ± ± 0.5 °C and stirred at 100 rpm. Aliquots of 5 mL were withdrawn at predetermined time intervals and replaced with equal amount of fresh dissolution medium. After suitable dilution, the samples were analyzed by HPLC method and cumulative percentage drug release (CPR) was calculated.

2.19. Principal component analysis

PCA was implemented to reveal latent structures in the data set and to identify grouping of the materials using The Unscrambler® 10.2 software (CAMO AS, Norway). The data matrix included the previously described set of materials (objects, = 14), each characterized by various parameters (variables, $p = 21$). PCA modeling was done using systematic cross-validation; data were centered and scaled using a common normalization method (1/SDev) (Esbensen, 2006). A systematic approach was applied; first, including pure RCD and agglomerates into the model, followed by identification of extremes or potential outliers. Extreme samples were then left out in order to analyze remaining materials in further detail.

3. Results and discussions

3.1. Preliminary investigations

3.1.1. Selection of solvent system

Agglomerates can be possible through the particular combinations of solvents. The selection of solvent system for agglomeration process depends on the solubility and stability of RCD in various solvents. Water has been reported as a processing (bad solvent/external phase) medium and organic solvents (relatively nontoxic) as a good solvent (internal phase) and/or bridging liquid in the system design for water insoluble drug. This method of solvent system selection has been implemented due to the scarce requirement of organic solvent as a good solvent as well as bridging liquid. The bridging liquid should carry out better wetting of crystalline drugs and form liquid bridges during the process of agglomeration. Simultaneously, bridging liquid should be immiscible with bad solvent to avoid drug loss due to co-solvency which subsequently improves the yield of the process. Based on this criteria various solvents were screened which includes water, ethanol, dichloromethane (DCM), acetone, methanol, benzene, chloroform, dimethyl formamide, ethyl acetate, hexane and toluene. Amount of bridging liquid required was decided by trial and error method. It has been observed that, addition of inadequate amount of bridging liquid showed under wetting of crystals resulting in generation of smaller size agglomerates with more number of fines. Whereas excess addition of bridging liquid generates bigger size agglomerates requiring more processing time for completion of agglomeration process. Solubility studies were carried out in selected solvents using Higuchi rotating bottle method (Batt and Garala, 2012) and results are illustrated in Fig. 1. Most works do not report the reasoning behind their solvent selection; Chow and Leung (1996) have found some general rules to select solvent system as a starting point. According to their principles, the water works well as a continuous phase for a water insoluble drug. As per drug solubility profile, RCD has the highest solubility in DCM and least solubility in water. Therefore, water was selected as a poor solvent for maximum recrystallization and DCM as good solvent to formulate agglomerates of RCD.

3.1.2. Selection of excipients and processing conditions

On the basis of solubility study, DCM and water were identified as good solvent and bad solvent, respectively for the preparation of the crystal-co-agglomerates of RCD. In the formulation of pharmaceutical dosage form various excipients are utilized to improve the

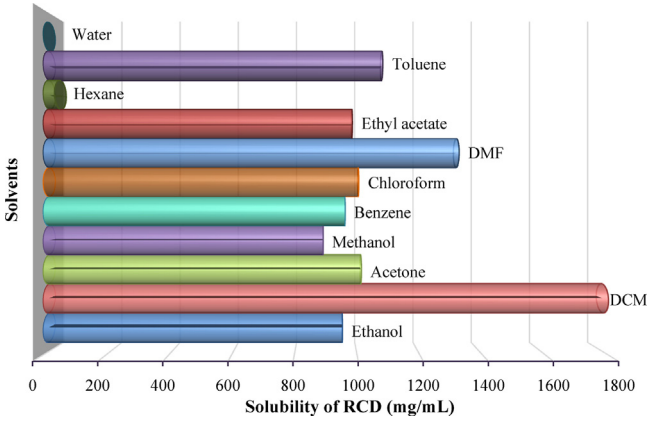

Fig. 1. Solubility profile of RCD in various solvents.

functionality of dosage forms. All these excipients have a significant impact on their bioavailability, toxicity, stability and efficacy (Zhenhao et al., 2011). Addition of small amounts of surfactants or polymers is the method usually applied to get the best spherical particles. Surfactants or polymers decrease the interfacial tension between fluids, change the viscosity of phases and hence influences the droplets sphericity (Teychene et al., 2010). The results of RCD agglomerates with all the studied excipients have been summarized in Table 2. A literature survey revealed the application of talc as inert diluent component (Lin and Peck, 1995) and it has been extensively used in the design of dosage forms. In the present investigation, talc was selected as an agglomerating agent which was able to generate miniscular form. Because of the hydrophobic nature of talc, it undergoes preferential wetting with non-aqueous solvent (DCM) which justified the suitability of it as an excipient for agglomeration. Results show that agglomerates obtained with talc at 1% w/w concentration (trial PR3) improves the functionality of RCD agglomerates (Table 2). Talc concentration below 1% produces agglomerates with poor characteristics and required more time to develop which may be attributed lack of ability to start the formation of miniscular form. Further, higher concentration (>1%) of talc results in very poor strength which may be because of weak bond formation and the least adsorption capacity (Ganjian et al., 1980). Therefore, 1% w/w talc was utilized for the formation of RCD agglomerates. This preliminary investigation, also revealed that the crystallization and agglomeration of pure drug (without excipients) exhibited poor handling qualities (Kawashima et al., 1984).

In addition, investigation revealed that the presence of polymers on the particle surface, which increases particle-particle interaction, may cause faster squeezing out of DCM to the surface, which results in particle size enlargement. Agglomeration was carried out by utilizing different concentration of PVP and HPC (trials PR6–PR13). However, for both the polymers the results of study parameters were unfavorable. This may be attributed to the polymer structure, structure compatibility in term of free availability of hydrophobic and hydrophilic group for interaction between polymer and drug, polymer molecular weight and viscosity (Kumar et al., 2008). Therefore, addition of PVP and HPC was not further justified for the preparation of RCD agglomerates. Furthermore, an agglomeration of RCD was also attempted with a hydrophobic polymer (EC). With respect to its high yield strength, EC on crystallization in non-solvents imparts more strength to the agglomerates (Jadhav et al., 2007). However, the agglomerates showed unfavorable characteristics which may be attributed to its solubility in the good solvent which imparts viscosity to the internal phase and increases interfacial tension (Pawar et al., 2004a; Hu et al., 2006). Due to failure of EC to enlarge particle size and improvement of flowability, it was not utilized for preparation of agglomerates.

Table 3
Selection of stirring speed for RCD agglomeration.

Trial	Speed (RPM)	Results[a]		
		dg (μm)	AoR (°)	CS (gm)
PR32	200	2427.1 ± 247.33	40.14 ± 3.17	17.15 ± 1.35
PR33	400	1902.5± 152.56	37.23 ± 1.43	29.33 ± 0.94
PR34	600	1267.6 ± 128.49	26.45 ± 1.65	38.54 ± 2.91
PR35	800	735.34 ± 50.88	18.56 ± 1.32	45.32 ± 2.73
PR36	1000	368.65 ± 32.95	23.81 ± 1.48	42.56 ± 1.31
PR37	1200	154.35 ± 24.67	21.44 ± 2.73	19.61 ± 0.43

[a] Results are mean of three observation ±SD.

Therefore, agglomerates tried with HPMC (1%) shows adequate mechanical strength, whereas excess addition of HPMC resulted in ellipticity and deformation of agglomerates (Paradkar et al., 2010). Hence, HPMC at 1% concentration was fixed for agglomerates of RCD. An emulsifier (PVA) was also tried to obtain the optimum distribution of globules during a process as reported earlier (Paradkar et al., 2003). PVA at a concentration below 1.5% exhibits wide particle size distribution due to poor globules distribution, whereas at higher concentration (>1.5%) PVA does not able to produce sufficient size enlargement with desired mechanical strength. Therefore, it was decided to add PVA in a concentration of 1.5% for all further trials of RCD agglomerates.

Up to here, the addition of various polymers in the crystallization process leads to the formation of agglomerates with improved functionality, but still appropriate sphericity was lacking. A literature survey has revealed the application of PEG as sphericity imparting agent (Jadhav et al., 2010). PEG caused a reduction in the interfacial tension between external phase (water) and internal phase (DCM) resulting in a reduction in the force of cohesion between particles leading to generation of small spherical agglomerates (Kawashima et al., 1986a, 1986b). PEG between 2 and 5% concentration imparts good sphericity to agglomerates which may be attributed toward reduced interfacial tension and favored wetting of drug particles. However, agglomerates prepared in the presence of PEG have low CS due to low adhesive force of PEG. Due to a soft and plastic nature of PEG, it undergoes plastic deformation and gives better compressibility to the agglomerates during the process of compression (Jadhav et al., 2007). Hence, PEG was selected in a concentration between 2 and 5% w/w.

Different agglomerates of RCD (trial PR32–PR37) were prepared to select the optimum speed of rotation (Table 3). When the agitation speed was reduced to 200–400 rpm, larger irregular agglomerates were obtained, where the shear energy may not be sufficient for the formation of spherical shape of agglomerated crystals. Agglomerates prepared at 600 rpm (trial PR34) results in a uniform size distribution. It appears to be clear that the optimum shear force of the agitated liquid and collisions with equipment (baffles) surfaces and other particles were squeezing and molding the irregular agglomerates into an almost perfect spherical shape (Thati and Rasmuson, 2011). The impact of agitation speed on the formation of spherical agglomerates was such that on further increasing the agitation speed beyond 1000 rpm, spherical agglomerates with smaller diameter (dg = 154.35 μm) were produced with poor CS. Additionally, there were fines present along with irregular shaped agglomerates, which could be due to high shear force of stirrer. Therefore, it was determined that the rotational speed between 600 and 1000 rpm was optimized by implementation of suitable design of experiment.

Temperature is a very critical factor in the formation agglomerates. The results depicted that at low (5 °C) temperature the agglomerates were bigger than at room temperature (28 °C) (Table 4). Because of the large size of prepared agglomerates of trial PR38, it was not further considered as processing temperature. This

Table 4
Selection of temperature for RCD agglomeration.

Trial	Temperature (°C)	Results[a]		
		dg (μm)	AoR (°)	CS (gm)
PR38	5	3027.3 ± 176.5	36.55 ± 2.12	17.15 ± 1.35
PR39	28	652.45 ± 20.17	24.64 ± 1.88	37.21 ± 2.42
PR40	40	206.85 ± 17.64	30.29 ± 2.06	10.43 ± 0.74
PR41	Good solvent, 40 Poor solvent, 10	432.61 ± 24.98	24.57 ± 1.21	11.28 ± 0.53

[a] Results are mean of three observation ±SD.

might be attributed to less solubilization of the drug would cause reduced wetting of drug particles and therefore, agglomerates obtained with poor mechanical strength (Gordonx and Chowhan, 1990). Further trial (PR39) carried out at room temperature results in agglomerates with good sphericity and strength. While at higher temperature (40 °C) agglomerates were not formed with desired size along with the generation of large amount of fines. This might be attributed to higher rates of evaporation of DCM which leads to later unavailability of bridging liquid to complete agglomeration of RCD. Further, this also leads to the low strength of agglomerates and breaking of agglomerates due to shear force of stirrer. The rate of crystallization was increased on temperature difference between good and poor solvent. On creating a temperature difference in solvents (trial PR41), agglomerates with good sphericity and uniformity were obtained but they possessed the very low strength. This might be attributed to the good solvent entrapment in a matrix which on drying evaporates and leads to a very porous structure which results in low strength to RCD agglomerates. Further continuous stirring results in fractured agglomerates which might be due to poor strength. Finally, it was decided that the temperature for the preparation of RCD agglomerates was most suitable at room temperature.

The phase ratio of good solvent (DCM) to poor solvent (water) altered the fundamental properties of RCD agglomerates (Table 5). In trial PR42 (phase ratio, 0.02), agglomerates were obtained with poor strength and irregular shape. It might be attributed to low amount of good solvent which leads to rapid evaporation and unable to make strong linkages between growing crystals. Also, generation of fines was observed due to the incomplete agglomeration of crystals. Further, trial PR43 revealed sufficient size enlargement and strength with improved flow properties. Also, increase in the phase ratio (trial PR47) results in formation of large size agglomerates with rough surface characteristics as well as unsatisfactory strength. These findings were due to the time required for evaporation of higher amount of solvent which leads to the loss of polymer during the process. Hence, on the basis of appropriate dg and AoR with high CS, phase ratio between 0.04 and 0.1 was selected for further investigation. At last in summary, 1% talc, 1% HPMC and 1.5% PVA were optimized for RCD agglomeration. In addition, PEG between 2 and 5%, the phase ratio (DCM: water) between 0.04 and 0.1 and stirring speed between 600 and 1000 rpm were selected as independent variables.

Table 5
Selection of phase ratio for RCD agglomeration.

Trial	Phase ratio (DCM: Water)	Results[a]		
		dg (μm)	AoR (°)	CS (gm)
PR42	0.02	421.36 ± 28.32	31.28 ± 1.34	23.27 ± 3.25
PR43	0.04	595.41 ± 58.04	28.75 ± 1.27	35.95 ± 4.21
PR44	0.06	648.29 ± 89.27	26.43 ± 2.59	42.53 ± 3.29
PR45	0.08	975.62 ± 102.21	23.48 ± 2.14	50.42 ± 3.74
PR46	0.10	1524.85 ± 245.8	23.21 ± 2.75	47.19 ± 2.25
PR47	0.12	2315.73 ± 426.2	34.26 ± 2.69	27.52 ± 3.36

[a] Results are mean of three observation ±SD.

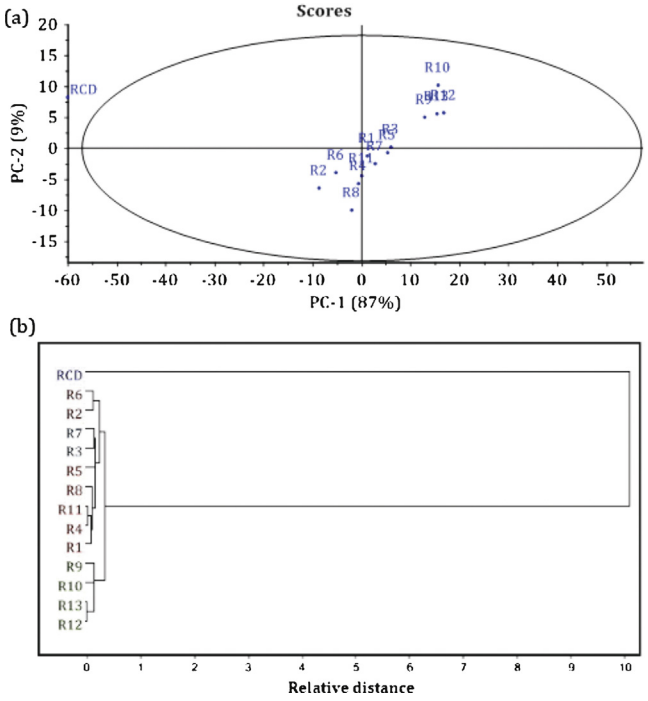

Fig. 2. Score plot from PCA (a) and Dendrogram from AHCA (b) of pristine and agglomerated RCD.

3.2. Principal component analysis

For all experimental design batches of RCD agglomerates, responses like percent yield (%*Y*), mean geometric diameter (dg), AoR, Carr's index (CI), Hausner ration (HR), drug content (DC), aspect ratio (φ), irregularity factor (IF), CS, shape factor (SF), circularity factor (CF), Kawakita parameters (a and $1/b$), Kuno's constant (K), Heckel plot parameters (A, k, Py and σ_o), elastic recovery (ER), tensile strength (TS) and MC were evaluated and documented in Table 6. PCA was performed on these data set using software package The Unscrambler® 10.2 for all experimental design batches in order to scrutinize critical responses.

The multivariate approach by using PCA dates back to the beginning of the 20th century (Pearson, 1901) and most common latent variable projection method (Rajalahti and Kvalheim, 2011). PCA is a mathematical algorithm that reduces the dimensionality of the data while retaining most of the variation in the data set (Ringer, 2008). It allows the results to be simplified into latent variables (principal components) that explain the main variance in the data (Haware et al., 2009). PCA is used for getting overview of data tables (their structure, similarities or dissimilarities, trends, deviating observations).

Initially, PCA was performed to examine the relationship of all properties obtained from the series of experimental design and untreated crystals of RCD. Further, identification of objects for the different developmental stages was carried out by examining the scores and the loadings. The loadings are the contributions from the variables to the principal components and the scores are the contributions from the samples. The larger the loading, the more important the agglomerates for a particular PC is; and the larger the score, the more important the sample is (Kubista et al., 2007).

As depicted in Fig. 2(a), the first principal component (PC1) was responsible for 87% of the total variance in the data set and the second (PC2) was responsible for a further 9%; thus, the

Table 6
Results of evaluation parameters of pristine and agglomerated RCD.

Batch*	RCD	R1	R2	R3	R4	R5	R6
dg[a] (mm)	0.137 ± 0.103	0.697 ± 0.142	0.892 ± 0.139	0.725 ± 0.127	0.973 ± 0.116	1.009 ± 0.168	1.214 ± 0.193
CS[b] (gm)	–	46.27 ± 3.66	35.41 ± 1.51	51.07 ± 2.69	42.18 ± 2.38	49.32 ± 2.75	39.24 ± 1.98
SF[c]	0.415 ± 0.052	0.826 ± 0.083	0.809 ± 0.067	0.901 ± 0.065	0.896 ± 0.073	0.938 ± 0.071	0.857 ± 0.053
CI[d]	39.48 ± 2.05	14.57 ± 1.29	17.84 ± 2.67	17.09 ± 1.68	15.43 ± 1.34	14.55 ± 1.06	17.73 ± 1.25
%Y[e]	–	94.59 ± 2.07	88.17 ± 2.66	90.43 ± 1.92	96.25 ± 1.43	98.16 ± 2.61	91.64 ± 2.75
AoR[f] (°)	45.63 ± 3.65	23.81 ± 1.38	22.94 ± 2.07	19.07 ± 1.76	20.18 ± 1.59	18.59 ± 1.67	22.45 ± 0.98
HR[g]	1.613 ± 0.132	1.141 ± 0.011	1.176 ± 0.013	1.165 ± 0.014	1.154 ± 0.012	1.150 ± 0.013	1.205 ± 0.027
CF[h]	0.354 ± 0.038	1.015 ± 0.271	0.973 ± 0.184	0.991 ± 0.143	0.987 ± 0.156	1.089 ± 0.117	1.107 ± 0.128
IF[i]	2.017 ± 0.073	2.936 ± 0.115	2.975 ± 0.129	3.024 ± 0.134	3.066 ± 0.128	2.891 ± 0.119	3.032 ± 0.083
Φ[j]	0.075 ± 0.012	0.856 ± 0.107	0.832 ± 0.083	0.907 ± 0.074	0.883 ± 0.051	0.940 ± 0.087	0.895 ± 0.075
DC[k] (%)	–	98.54 ± 1.62	99.35 ± 1.75	95.67 ± 1.23	100.23 ± 1.07	97.84 ± 1.68	97.17 ± 1.64
MC[l] (%)	0.324 ± 0.101	0.735 ± 0.134	0.864 ± 0.153	1.113 ± 0.203	1.011 ± 0.196	0.996 ± 0.173	0.965 ± 0.135
a[m]	17.455 ± 1.06	5.154 ± 0.638	9.457 ± 0.921	5.181 ± 0.315	5.378 ± 0.423	4.735 ± 0.437	6.348 ± 0.539
$1/b$[m]	1.375 ± 0.073	0.752 ± 0.064	0.528 ± 0.027	0.441 ± 0.092	0.541 ± 0.078	0.994 ± 0.083	0.645 ± 0.035
K[n]	0.079 ± 0.015	0.974 ± 0.093	0.953 ± 0.084	0.931 ± 0.102	0.987 ± 0.113	1.025 ± 0.132	0.983 ± 0.064
A[o]	1.375 ± 0.073	0.752 ± 0.064	0.528 ± 0.027	0.441 ± 0.092	0.541 ± 0.078	0.994 ± 0.083	0.645 ± 0.035
k[o]	0.079 ± 0.015	0.974 ± 0.093	0.953 ± 0.084	0.931 ± 0.102	0.987 ± 0.113	1.025 ± 0.132	0.983 ± 0.064
Py[o] (tons)	29.24 ± 1.83	1.711 ± 0.09	1.739 ± 0.12	2.020 ± 0.22	1.594 ± 0.08	1.516 ± 0.09	1.639 ± 0.17
σ_o[o]	9.746 ± 1.02	0.570 ± 0.16	0.579 ± 0.19	0.673 ± 0.17	0.531 ± 0.15	0.505 ± 0.18	0.546 ± 0.12
ER[p] (%)	4.453 ± 0.497	0.815 ± 0.165	0.731 ± 0.234	0.725 ± 0.186	0.697 ± 0.127	0.554 ± 0.201	0.735 ± 0.179
TS[q] (kg/cm^2)	1.253 ± 0.131	5.215 ± 0.652	4.942 ± 0.341	5.697 ± 0.763	6.015 ± 0.434	4.684 ± 0.372	5.248 ± 0.421

Batch*	R7	R8	R9	R10	R11	R12	R13
dg[a] (mm)	0.351 ± 0.083	0.723 ± 0.091	1.102 ± 0.104	1.175 ± 0.157	0.437 ± 0.113	0.566 ± 0.115	0.834 ± 0.138
CS[b] (gm)	47.01 ± 2.65	38.44 ± 2.83	58.89 ± 3.61	64.35 ± 3.89	43.73 ± 2.37	62.98 ± 3.95	61.58 ± 3.52
SF[c]	0.992 ± 0.084	0.970 ± 0.077	0.792 ± 0.052	0.876 ± 0.047	0.841 ± 0.061	0.912 ± 0.043	0.959 ± 0.051
CI[d]	16.33 ± 1.78	15.61 ± 0.92	14.05 ± 0.83	15.84 ± 1.29	15.56 ± 1.15	14.24 ± 0.83	14.74 ± 0.73
%Y[e]	91.07 ± 2.94	96.65 ± 1.32	97.35 ± 2.73	92.17 ± 1.61	89.83 ± 1.36	93.55 ± 2.83	97.23 ± 2.97
AoR[f] (°)	17.84 ± 1.32	17.06 ± 2.17	17.51 ± 1.38	21.23 ± 1.52	22.35 ± 1.13	18.97 ± 1.39	18.41 ± 1.26
HR[g]	1.154 ± 0.016	1.144 ± 0.015	1.096 ± 0.011	1.155 ± 0.014	1.143 ± 0.012	1.136 ± 0.011	1.128 ± 0.013
CF[h]	0.999 ± 0.135	0.989 ± 0.113	0.982 ± 0.126	0.974 ± 0.149	0.987 ± 0.134	0.993 ± 0.148	1.054 ± 0.117
IF[i]	3.112 ± 0.201	2.959 ± 0.124	2.872 ± 0.139	2.983 ± 0.097	3.013 ± 0.133	3.047 ± 0.116	2.981 ± 0.124
Φ[j]	0.999 ± 0.054	0.981 ± 0.037	0.728 ± 0.056	0.868 ± 0.048	0.876 ± 0.074	0.912 ± 0.063	0.965 ± 0.055
DC[k] (%)	98.42 ± 2.09	99.68 ± 1.48	97.75 ± 1.96	98.23 ± 1.93	101.03 ± 1.61	99.58 ± 1.37	98.24 ± 1.46
MC[l] (%)	0.935 ± 0.158	0.918 ± 0.127	0.815 ± 0.139	0.997 ± 0.162	0.834 ± 0.137	1.017 ± 0.193	0.973 ± 0.175
a[m]	9.366 ± 0.832	2.854 ± 0.261	7.656 ± 0.733	5.335 ± 0.342	2.806 ± 0.303	2.847 ± 0.376	3.739 ± 0.294
$1/b$[m]	0.814 ± 0.054	0.969 ± 0.032	0.796 ± 0.051	0.640 ± 0.072	0.514 ± 0.061	0.624 ± 0.049	0.756 ± 0.051
K[n]	1.214 ± 0.083	0.995 ± 0.097	0.953 ± 0.108	0.941 ± 0.093	1.106 ± 0.112	0.967 ± 0.094	0.985 ± 0.082
A[o]	0.814 ± 0.054	0.969 ± 0.032	0.796 ± 0.051	0.640 ± 0.072	0.514 ± 0.061	0.624 ± 0.049	0.756 ± 0.051
k[o]	1.214 ± 0.083	0.995 ± 0.097	0.953 ± 0.108	0.941 ± 0.093	1.106 ± 0.112	0.967 ± 0.094	0.985 ± 0.082
Py[o] (tons)	1.971 ± 0.09	1.437 ± 0.07	1.806 ± 0.15	1.462 ± 0.06	1.421 ± 0.07	1.208 ± 0.06	1.367 ± 0.08
σ_o[o]	0.656 ± 0.13	0.479 ± 0.11	0.604 ± 0.17	0.487 ± 0.15	0.473 ± 0.14	0.402 ± 0.16	0.455 ± 0.17
ER[p] (%)	0.836 ± 0.193	0.565 ± 0.152	0.468 ± 0.103	0.578 ± 0.118	0.549 ± 0.134	0.605 ± 0.156	0.765 ± 0.149
TS[q] (kg/cm^2)	5.367 ± 0.587	6.164 ± 0.832	5.654 ± 0.426	4.964 ± 0.319	5.548 ± 0.571	5.218 ± 0.385	5.584 ± 0.463

[a] Mean geometric diameter.
[b] Crushing strength.
[c] Shape factor.
[d] Carr's Index
[e] Percent yield.
[f] Angle of repose.
[g] Hausner ratio.
[h] Circularity factor
[i] Irregularity factor.
[j] Aspect ratio.
[k] Drug content.
[l] Moisture content.
[m] Kawakita parameters.
[n] Kuno's constant.
[o] Heckel parameters.
[p] Elastic recovery.
[q] Tensile strength.
* Results are mean of three determinations ±SD.

cumulative contribution was 96%. Based on the PCA score plot in Fig. 2(a), RCD crystal was categorized as extreme objects. The RCD was separated from the agglomerates of all 13 batches as clearly observed outside of eclipse, which was further proved by AHCA. AHCA refers to a set of analytical procedures that reduce complex multivariate data into smaller subsets or groups (Singh et al., 2010). Compared with other data reduction methods, AHCA yields groupings that are based on the similarity or dissimilarity of whole cases (Dai et al., 2012). AHCA represents a valuable analytical tool and may be used to devise patient or consumer profiles, or in the development of classification systems or taxonomies. The data obtained were also classified by AHCA using the Euclidean distance (nearest neighbor method) (Cutrignelli et al., 2008). Euclidean distances, which can reveal the relationship of two samples, are calculated by equation (15).

$$\text{EUCLID} = \sqrt{\sum_{i=1}^{n} (x_i - y_i)^2} \quad (15)$$

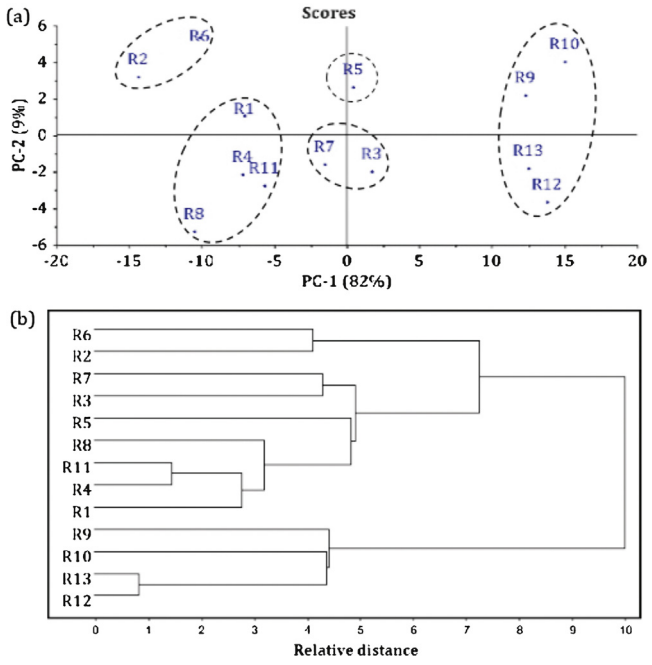

Fig. 3. Score plot from PCA (a) and Dendrogram from AHCA (b) of agglomerated RCD.

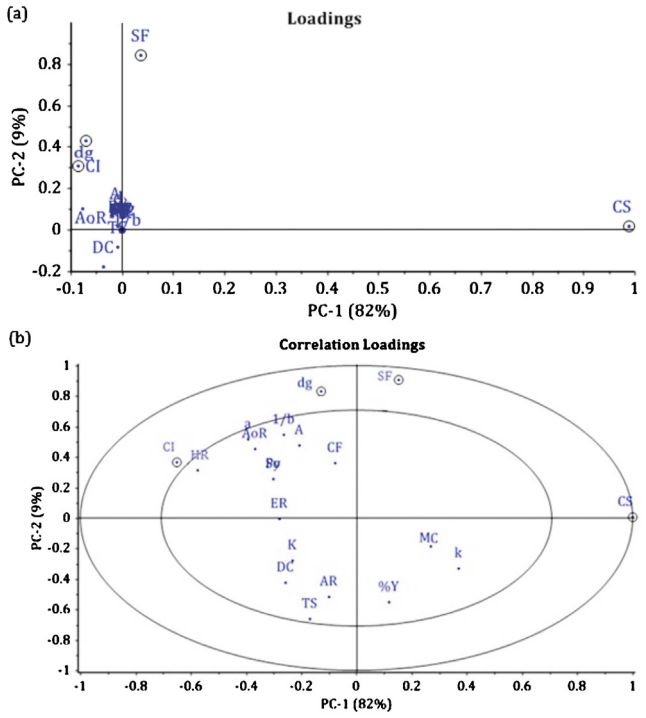

Fig. 4. Loading (a) and Correlation loading (b) plot obtained by PCA of RCD agglomerates' properties.

EUCLID is Euclidean distances of two samples; n is number of variables, x_i is value of variable i of one sample, y_i is value of variable i of another sample. Then cluster analysis diagram can be obtained by Euclidean distances (Chen et al., 2006).

Furthermore, resulting PC scores were analyzed by a clustering approach. This approach is often considered an optimal way to perform classifications. With hierarchical average linkage, which is an agglomerative method, each samples (as represented by its component scores) initially started out as an individual cluster. Similar agglomerates were then merged, where cluster similarity was determined by the mean distance between all objects in the clusters (weighted by the number of members), until all samples were united into one cluster (Xu and Redman-Furey, 2007). The AHCA results were examined in the form of a dendrogram (a tree of clusters) and subjectively determine how many clusters appear to exist with their similarities (Leonard and Droege, 2008).

The dendrogram, a graphical display of the result of AHCA is shown in Fig. 2(b). Two major clusters were found representing coarse RCD and agglomerated RCD batches separately with higher relative distance. It revealed that various properties of coarse RCD were significantly distinctive from agglomerated RCD. This finding proved the results of PCA score plot (Fig. 2(a)). Therefore, RCD was eliminated from the data set and a new PCA model was built without RCD, as a means to better illustrate the distribution of the remaining agglomerated RCD.

The PCA score plot of all the variables of 13 batches of Box–Behnken design is given in Fig. 3(a). The agglomerates spread out relatively homogeneously into four quartiles of the score plot and the PC1 was responsible for the largest variation, i.e. 82%, of the total variance in the data set, while the PC2 was responsible for a further 9%; thus, the cumulative contribution was 91%. Further, all 13 batches of experimental design were defined in different group by AHCA. It was used for evaluation of the similarity and dissimilarity of all batches. As seen from Fig. 3(b), all the formulations were clustered into five groups; group I (R2 and R6), group II (R3 and R7), group III (R5), group IV (R1, R4, R9 and R11) and group V (R9, R10, R12 and R13). All the five groups were relatively distant and substantially different from one another.

Loading plot of the first two principal components is shown in Fig. 4(a). In general, it is considered that variables near each other are positively correlated, while those on opposite sides of the origin are negatively correlated in loading plots. All defined properties of agglomerates were classified into following four groups based on the origin; top, bottom, right and left. With regard to the variables, dg and CS were plotted on opposite sides of the origin while SF and CS were plotted in similar positions. Therefore, CS was found to be negatively correlated with dg and CS was positively correlated with SF. This result implied that if the dg of agglomerates was improved, the CS would decrease. In addition, the SF and AoR were negatively correlated with CI. This finding suggests that as sphericity of agglomerated RCD increases, flow parameters (AoR and CI) decreases and ultimately improved flowability. Again, this result correlates with previous investigation (Liu et al., 2008). Other variables, dg and SF oppositely plotted in loading plot indicated that with increase in size of agglomerates, sphericity would be disturbed. Moreover, other variables plotted on loading plot were at very low values near to origin and hence, it was not further considered for discussion. Finally, this PCA result was also considered to be reasonable and the cumulative contribution ratio of PC1 and PC2 was 91%. Correlation loading plot was also constructed to decide most important variables for further optimization. Correlation loading plot is seen in Fig. 4(b) depicts the four most important variable (marked by a circle) as they enclosed between two eclipse.

Fig. 5 shows a PCA bi-plot containing both scores and loading vectors of agglomerates. In the PCA bi-plot, CS of batch R9, R10, R12 and R13 were plotted on same side of PC1, it depicted that they are positively correlated and hence, CS of these batches was high. In Fig. 6, the third principal component (PC3), explaining an additional 4% of the variation in the data, is displayed in 3D plot against PC1 and PC2. Due to very low explained variation of PC3, it was not important in development of agglomerates and hence, not further discussed. The reduced PCA model was explained a total of 95% of the variation on the data set over three principal components (PC1: 82%; PC2: 9%; PC3: 4%).

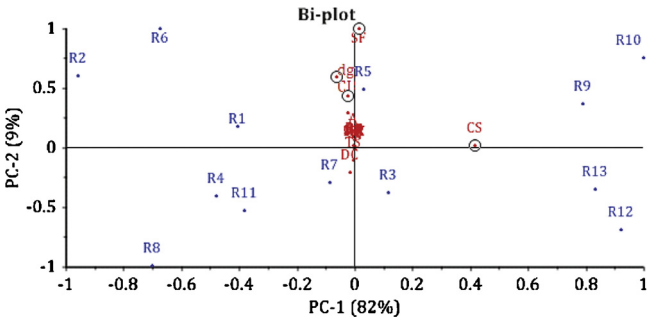

Fig. 5. Bi-plot obtained by PCA of RCD agglomerates.

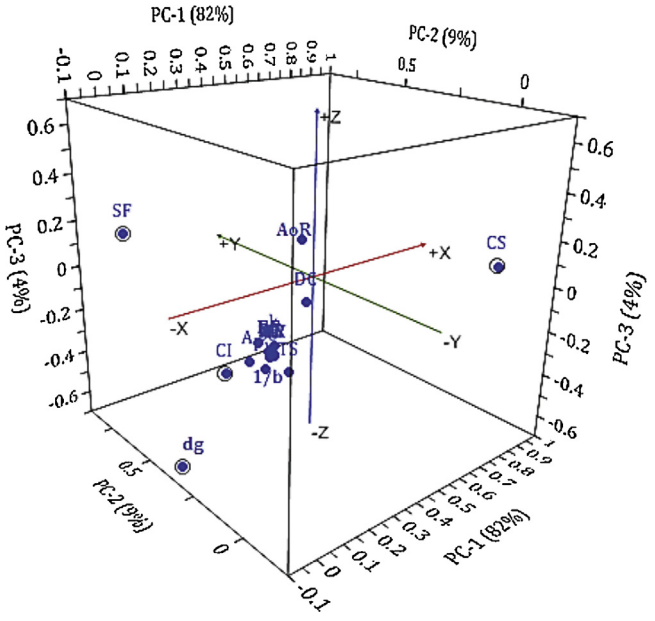

Fig. 6. PCA 3D loadings plot for the PC1, PC2 and PC3.

Plotting the eigenvalues against the corresponding PC produces a scree plot that illustrated the rate of change in the magnitude of the eigenvalues for the PC. The Cattell (1966) scree test and the Kaiser (1960) criterion are the most frequently used procedures. They are both based on inspection of the correlation matrix eigenvalues. Cattell's recommendation was to retain only those components above the point of inflection on a plot of eigenvalues ordered by diminishing size. Kaiser (1960) recommended that only eigenvalues at least equal to one are retained as one is the average size of the eigenvalues. Eigenvalues of all PCs were calculated using XLSTAT® software version 2008.6.03 (Addinsoft, Italy). The scree plot shown in Fig. 7 displays the eigenvalues for each

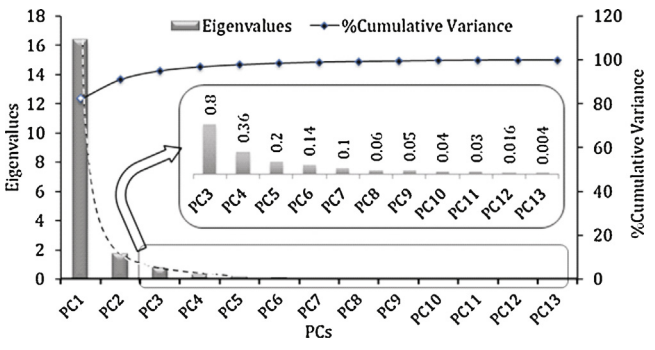

Fig. 7. Scree plot of all components with cumulative variance.

component in descending order. The aim was to look for a "large gap" or and "elbow" in the graph. The rate of decline tends to be fast initially then levels off. The 'elbow', or the point at which the curve bends (dotted line in Fig. 7), was considered to indicate the maximum number of PC to extract. This scree plot revealed that there was one large gap/break in the data between components 1 and 2 and then the eigenvalues begins to flatten out beginning with component 3. This indicated that only these two components (1 and 2) should be retained and interpreted. A sequential analysis may likely show the components 3–13 appear after the break and were assumed to be trivial and hence not retained. Also eigenvalues of components 3–13 were less than unity (1) and can therefore be neglected and not interpreted (Zhu and Ghodsi, 2006). From the percentage cumulative variance plot (Fig. 7), it appears to be 2 "dimensional" represented by components 1 and 2 that accounts for 91% of the variation in the data. Thus, it was considered that the dg, CI, SF and CS were the most important variables in the preparation of superior agglomerates of RCD and hence, they were further selected for the optimization.

3.3. Optimization of agglomerates

For all the 13 batches of experimental design, selected dependent variables [mean geometric diameter (Y_1), CS (Y_2), shape factor (Y_3) and Carr's index (Y_4)] exhibited wide variations from 0.351 to 1.214 mm, 35.41 to 64.35%, 0.7925 to 0.9922 and 14.29 to 17.84, respectively (Table 6). The data clearly indicated strong influence of selected factors (X_1, X_2 and X_3) on responses (Y_1, Y_2, Y_3 and Y_4). The polynomial equations was used to draw conclusions after considering magnitude of coefficients and mathematical sign it expresses either positive or negative (Table 7).

Using 5% significance level, a model was considered significant if the *P*-value (significance probability value) was less than 0.05 (Shah et al., 2007). For mean geometric diameter (Y_1), coefficients b_2, b_{12}, b_{23}, b_{13}, b_{23}, b_{11}, b_{22} and b_{33} were found to be insignificant ($P > 0.05$) and therefore, these terms were separated from their full model in order to develop reduced model regression equations. Similarly, the coefficient (marked with "C″) in Table 7 were found to be insignificant ($P > 0.05$) for CS (Y_2), shape factor (Y_3) and Carr's index (Y_4) and hence, these terms were removed from their respective full model in order to develop reduced model regression equations (Singh et al., 2005a). The removal of insignificant terms was further justified by executing analysis of variance (ANOVA) test (Table 8). In this experiment, high value of correlation coefficients for all the selected dependent variables i.e., Y_1, Y_2, Y_3 and Y_4 illustrates goodness of fit. This was an inference of validation of reduced model (Shah et al., 2007).

The fitted model, for Y_1, was evaluated using priori linearity hypothesis test (Faria et al., 2011) and the results indicated that no evidence of lack of fit was observed in the 95% confidence interval, because calculated *F* value (Fcal) was 1.6816 and lower than their critical/tabulated value (Ftab) which was 8.89 (Zidan and Mokhtar, 2011). Likewise, for response Y_2, Y_3 and Y_4, calculated *F* values was less than their respective critical values (at $\alpha = 0.05$) which suggested insignificant difference amongst full and reduced model. The data of all the 13 batches of experimental design were used to generate interpolated values with the assistance of contour and perturbation plots (Mashru et al., 2005).

3.3.1. Influence of formulation composition on mean geometric diameter (Y_1)

The results of regression analysis for Y_1 depicted positive sign for regression coefficients b_1 and b_2 whereas it offered negative signs for coefficients b_3.This suggested that with increase in ratio of DCM to water with concentration of PEG 6000 and decrease in rotational speed (rpm) the mean geometric diameter (dg) of RCD

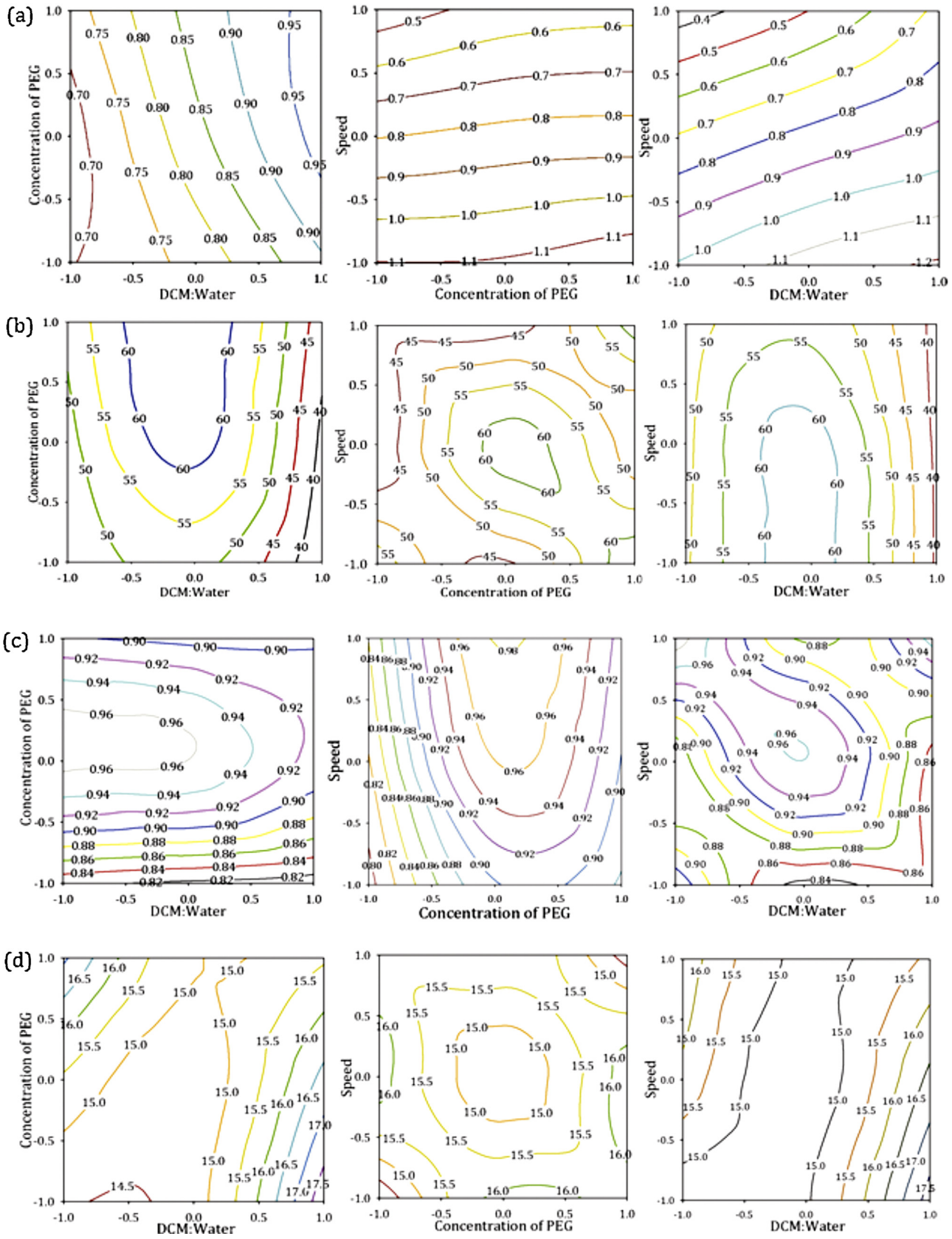

Fig. 8. Influence of formulation variables DCM: water (X_1), concentration of PEG 6000 (X_2) and speed (X_3) on dg (a), CS (b), SF (c) and CI (d) of RCD agglomerates by contour plot.

Table 7
Regression analysis of Box–Behnken design batches of RCD agglomerates.

Coefficients	dg (Y_1)		CS (Y_2)		SF (Y_3)		CI (Y_4)	
	FM[a]	RM[b]	FM	RM	FM	RM	FM	RM
b_0	0.834	0.823	47.32	47.45	0.959	0.943	14.7	14.87
b_1[c]	0.127	0.127	−11.15	−11.15	−0.016	–	0.51	0.51
b_2[c]	0.039	–	3.31	3.31	0.039	0.039	0.07	–
b_3	−0.303	−0.303	−0.50	−0.50	0.031	0.031	−0.05	−0.05
b_{12}[c]	0.013	–	−0.92	−0.92	0.003	–	−1.23	−1.23
b_{23}[c]	0.014	–	0.08	–	−0.003	–	−0.78	−0.78
b_{13}[c]	0.042	–	−0.24	–	0.015	–	−0.98	−0.98
b_{11}[c]	−0.004	–	1.32	1.27	−0.008	–	1.33	1.26
b_{22}[c]	−0.008	–	0.32	–	−0.093	−0.086	0.20	–
b_{33}[c]	−0.006	–	−0.15	–	−0.012	–	0.02	–

[a] FM, Full model.
[b] RM, Reduced model.
[c] Non-significant ($P > 0.05$) coefficients.

Table 8
Calculation for testing the model in portions for agglomerates of RCD.

Model	df[c]	SS[d]	MS[e]	R^2
		Mean geometric diameter (Y_1)		
Regression				
FM[a]	9	0.8846	0.0982	0.9941
RM[b]	2	0.8639	0.4319	0.9708
Residual				Fcal = 1.6816
				Fcritical = 8.89
				df = (7, 3)
FM	3	0.0052	0.0017	
RM	10	0.0259	0.0026	
		Shape factor (Y_2)		
Regression				
FM	9	0.0468	0.0052	0.9651
RM	3	0.0435	0.0145	0.8978
Residual				Fcal = 0.9628
				Fcritical = 8.94
				df = (6, 3)
FM	3	0.0016	0.0005	
RM	9	0.0049	0.0005	
		Crushing strength (Y_3)		
Regression				
FM	9	1093.828	121.5365	0.9998
RM	5	1093.084	218.6168	0.9991
Residual				Fcal = 2.9298
				Fcritical = 9.12
				df = (4, 3)
FM	3	0.1905	0.0635	
RM	7	0.9350	0.1335	
		Carr's index (Y_4)		
Regression				
FM	9	19.5088	2.1676	0.9941
RM	6	19.3587	3.2264	0.9864
Residual				Fcal = 1.2956
				Fcritical = 9.28
				df = (3, 3)
FM	3	0.1158	0.0386	
RM	6	0.2659	0.0443	

[a] FM, Full model.
[b] RM, Reduced model.
[c] df, Degree of freedom.
[d] SS, Sum of squares.
[e] MS, Mean of squares.

agglomerates increased. A highest dg of 1.214 was observed in batch R6 with levels of X_1, X_2 and X_3 as 1, 0 and −1, respectively. The contour plots corresponding to Y_1 are illustrated in Fig. 8(a). From the contour plot it is clear that increased DCM: water ratio and PEG 6000 concentration increased the response, dg. Additionally, it was also found that PEG has little positive effect on dg because of low coefficient value ($b_2 = 0.039$) whereas comparative high magnitude of DCM: water ($b_1 = 0.127$) indicates the more positive effect on dg (Table 7). It was mainly because higher amount of DCM serve as good bonding of crystals and ultimately increasing in size (Kawashima et al., 1982a,b). Also increase in the agglomerates size with increase in PEG 6000 concentration might be attributed to the ability of PEG 6000 to bind the growing crystals during process. Further, speed was highly influenced on dg as it showed high magnitude of negative coefficient ($b_3 = -0.303$). This might be due to higher amount of shear generated at elevated speed which ultimately reduced size of agglomerates.

As the number of response surface methodology (RSM) factors increased, it became difficult to visualize the response surface with graphical tools. In this case it is helpful to view a special form of response plot called "perturbation" for RSM data. Perturbation plots compared the effect of all the factors at a particular point in the RSM design space. The response was plotted by changing only one factor over its range, while holding all other factors constant. On the perturbation plot, a steep slope or curvature in an input variable indicates a relatively high sensitivity of response. Perturbation plot in Fig. 9(a) illustrated the effect of X_1, X_2 and X_3 variables on the dg. Extremely reduction in dg (high negative slope) was observed with increasing X_3 whereas slightly increase in dg was observed as the PEG 6000 concentration (X_2) increased. Also dg was incresed with X_2. These outcomes validate the regreession analysis (Table 7) and also confirmed the findings of counter plot (Fig. 8(a)).

3.3.2. *Influence of formulation composition factor on CS (Y_2)*

Randomly selected agglomerates from each batch were subject to CS determination. The total weight of mercury and weight of plunger to fracture/deform agglomerate was considered as CS. The results of regression analysis for CS (Y_2) depicted positive sign for regression coefficients b_2 whereas it offered negative sign coefficients b_1 and b_3 (Table 7). This indicated that with decreased DCM: water ratio along with speed and increased concentration of PEG 6000, the CS increased (Fig. 8(b)). Perturbation plot (Fig. 9(b)) also showed that CS increased with increased PEG concentration (X_2). This might be attributed to formation of strong matrix and uniformly bounded crystals to growing surface of agglomerates which leads to increase in CS.

Further, increased DCM: water (X_1) from −1 to 0 resulted in increased CS followed by decreased CS from level 0 to 1. This may be due to higher X_1, in this case above level 0, more time required to complete evaporation of DCM leads to loss of strength imparting polymer HPMC and, to a lesser extent, PEG during crystallization process and lower viscosity of droplets (Paradkar et al., 2002). Similarly negative regression coefficient value of b_3 indicated increased in CS with decrease in speed. It may be due to higher impact of growing agglomerates to each other and/or to the side wall of crystallization vessel at elevated speed. The results of

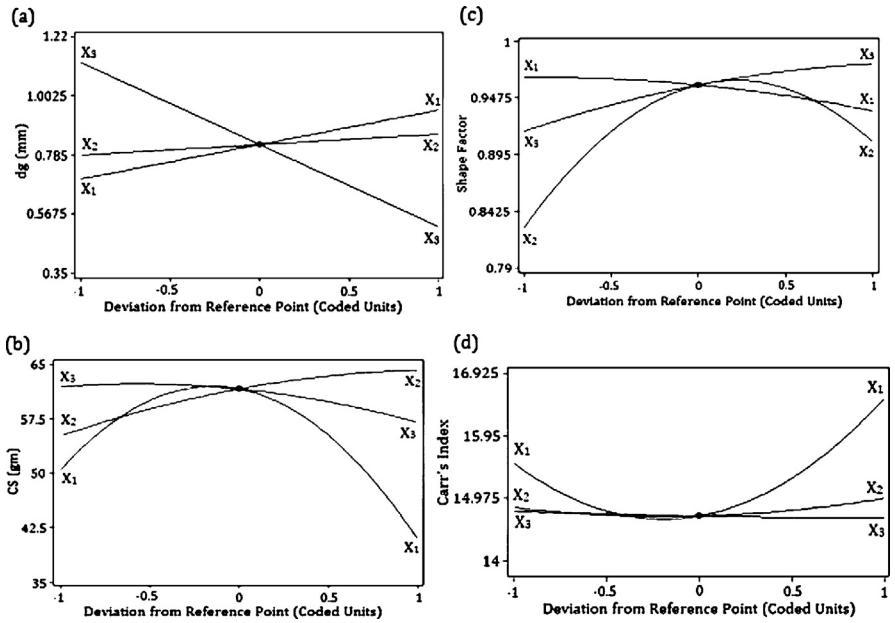

Fig. 9. Perturbation plots showing effect of independent factors on dg (a), CS (b), SF (c) and CI (d) of RCD agglomerates while keeping other variables at their respective midpoint.

CS of agglomerates showed that presence of excipients improved strength of agglomerates. This could be attributed to increased agglomeration of crystals with good bridging due to presence of suitable additives. Improved CS of agglomerates revealed the improvement in mechanical and handling properties. Increased cohesive interaction between particles caused better binding and close packing between crystals (Pawar et al., 2004b). A highest CS of 64.35 g was observed with batch R10 which has X_1, X_2 and X_3 at level of 0, 1 and −1, respectively.

3.3.3. Influence of formulation composition factor on shape factor (Y_3)

The results of regression analysis for Y_3 depicted positive sign for regression coefficients b_2 and b_3 whereas it offered negative sign for coefficients b_1. This suggested that with decreased ratio of DCM to water and increased concentration of PEG 6000 as well as rotational speed the shape factor (SF) of RCD agglomerates increased. A highest SF of 0.9922 was observed in batch R7 with levels of X_1, X_2 and X_3 as −1, 0 and 1, respectively. The results of contour plots are illustrated in Fig. 8(c). From the contour plots it is clear that increasing PEG 6000 concentration and rotational speed increases the SF, eventually sphericity of agglomerates. Additionally, high magnitude of regression coefficient b_2 (0.039) indicated PEG had positive influence on sphericity of RCD agglomerates (Table 7). PEG 6000 was the crucial polymer which could alter the crystal habit and the manner in which drug got recrystallized by giving a spherical shape. This may be attributed to adsorption of PEG 6000 at the growing surface of agglomerates and controlling or blocking the rate/growth of crystal formation (Jadhav et al., 2010; Ribardiere et al., 1996). In Fig. 9(c), perturbation plot revealed that, PEG 6000 only increased the sphericty at level −1 to 0.3, above 0.3 spericity started to decline as high concentration of PEG 6000 increased the viscosity of external phase that affects the size and distribution of globules. Further, reduction of sphericity was observed with increased DCM: water. This may be due to rapid evaporation of good solvent which produced agglomerates with uneven deposition of crystals on growing surface produced irregular shape agglomerates. From the perturbation plot (Fig. 9(c)), it was observed that with increasing the speed from −1 to 1 contributed in improving the sphericity of agglomerates.

3.3.4. Influence of formulation composition factor on Carr's Index (Y_4)

The results of regression analysis for Y_4 described positive sign for regression coefficients b_1 and b_2 whereas it offered negative sign for coefficients b_3 (Table 7). This suggested that with increased ratio of DCM to water, concentration of PEG 6000 and decreased in rotational speed the CI of RCD agglomerates increased. These results are illustrated as contour plots in Fig. 8(d).

Perturbation plot depicted that X_1 influences strongly on CI and it was confirmed by high magnitude of regression coefficient b_1 (0.51). Curve corresponding to X_1 declines from −1 to −0.3 and then rises gradually up to level 1, indicating that at low level of DCM: water the CI decreased and the flowability of agglomerates was improved. While higher amount of DCM reduced the sphericity of prepared agglomerates as it imparted roughness to the surface of growing agglomerates. Surface roughness affected sliding of the particles against each other, leading to difference in their packing geometry and thus, CI also. Hence, interparticle friction (due to roughness of the surface) appeared to influence the initial particle rearrangement, which might be a reason of increased CI as X_1 increased (Maghsoodi et al., 2007; Mahmoodi et al., 2010). Further, lower magnitude of regression analysis for X_2 and X_3 ($b_2 = 0.07$ and $b_3 = -0.05$) shows the lesser impact on CI and this was also confirmed from perturbation plot (Fig. 9(d)).

The optimized formulation was obtained by applying constraints on dependent variable responses and independent variables (Pattnaik et al., 2011). The constraints were: minimal CI; maximum CS; dg in range of 0.5–1 (mm) and SF target to 1. These constrains were common for all the formulations. The recommended concentrations of the independent variables were calculated by the Design Expert® version 7.1.5 (Stat-Ease, Inc., MN, USA) software from the overlay plot (Fig. 10) which has the highest desirability. The optimum values of selected variables obtained were −0.17 (X_1; DCM: water), 0.36 (X_2; concentration of PEG 6000) and 0.37 (X_3; speed). The final optimized composition of RCD agglomerates comprised of 0.065 DCM: water, 4.04% PEG 6000, 1%

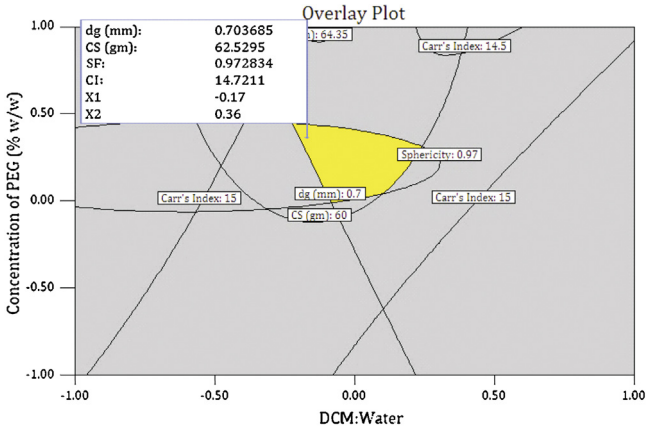

Fig. 10. Overlay plot for optimized parameters of RCD agglomerates.

talc, 1% HPMC E50LV and 1.5% PVA which was prepared by stirring at 874 rpm at room temperature.

Check point/optimized batch of RCD agglomerates (RO) was prepared according to the levels of factors optimized. The results depicted nonsignificant ($P > 0.05$) difference and lower magnitude of % relative error between experimentally obtained and theoretically computed data of dg, CS, SF and CI (Singh et al., 2005b) as well as significant values of R^2 (Roy and Shahiwala, 2009) suggested the robustness of mathematical model and high predictive ability of RSM applied (Table 9).

3.4. Percentage yield and drug content

Almost all the batches of agglomeration showed drug content (loading) >95%. The results indicated good loading efficiency and insignificant drug loss which was mainly because of slight solubility of drug in poor solvent. The % yield of prepared agglomerates is shown in Table 6. The percentage yield of agglomerated crystals was found in the range of 88.17–98.16%. The variation in % yield might be attributed to drug loss during agglomeration. During stirring the drug sticks to the wall of the vessel and remains unagglomerated.

3.5. Shape analysis

Aspect ratio (φ), shape factor (SF) and circularity factor (CF) for prepared agglomerates varies between 0 and 1, with low value indicating an elongated particle. A perfect sphere had an aspect ratio of 1, as seen in Table 6, the value of these descriptors near to unity. Irregularity of shape gave an indication of whether or not the particles were elongated or irregular. Irregularity measures the surface area compared to the size of the particle. A perfect circle has an irregularity of π. Low value of IF of RCD crystals (2.017 ± 0.281) is an indication of elongated particle shape. Value of IF of optimized RCD agglomerates was found to be 3.095 (± 0.127) indicating perfect spherical structure of agglomerates and it was confirmed from SEM. Elongated or irregular particles might tend to mechanically interlock or entangle with each other, thus obstructing powder flow and reducing flowability (Wouters and Geldart, 1996). Considering the shape parameters in combination can give more detailed information. For instance, prepared RCD agglomerates by CCA were more spherical in shape whereas RCD crystals were elongated and irregular in silhouette. The majority of drugs, including RCD, do not present adequate flow properties and high compressibility necessary for direct compression, requiring addition of excipients, which strengthens the weak linking between particles, facilitating the cohesion of the materials and, consequently, the compression (Sobrinho et al., 2008).

Table 9
Results of optimized batch (RO) of RCD agglomerates.

Response	Predicted value	Experimental value[a]	% Relative error
dg (mm)	0.7036	0.7312 ± 0.0216	3.92
CS (gm)	62.529	59.214 ± 1.8411	5.31
SF	0.9728	0.9615 ± 0.0632	1.16
CI	14.721	15.268 ± 0.8357	3.71

[a] Values are of mean of three observations ±SD.

3.6. Flowability measurements

The widespread use of solids in industries associated with agricultural, food, chemical, ceramic, pharmaceutical, metallurgical, and other bulk solids and powder processing has generated a variety of methods for characterizing flow behavior of solids. Improved processability refers to any advancement, which would facilitate downstream dosage form development or packaging, such as improved flowability and compressibility (Rogers and Wallick, 2012). Flow is defined as the relative movement of a bulk of particles among neighboring particles, or along the wall surface of a container (Ganesan et al., 2008). Poor flow properties affect adversely the ability to process such materials, for example, by hindering the mixing process and potentially affecting process performance (Pingali et al., 2008). Certain pharmaceutical solids often clump together and form cakes when it is stored for a long time. These clumps are sometimes very hard to break and often lead to damage to storage structures and economic losses (due to the use of sledgehammers and labor – time and salaries). To ensure steady and reliable flow, it is crucial to accurately characterize the flow behavior of these materials. As shown in Table 6, flow property of agglomerates obtained in the presence of excipients was excellent compared to RCD.

AoR gives a reproducible numerical value, so it has been adopted as a common method to assess flow properties mainly by the pharmaceutical industries (Craik and Miller, 1958). Lower AoR correspond to free flowing powders, whereas higher angles indicate a cohesive or poor flowing material (Cain, 2002). Remarkable reduction in AoR of agglomerates compared to pure drug indicated substantial improvement in flow and packing ability of agglomerates. CI empirically estimates the powder flow from packing density and compressibility. All the batches of prepared agglomerates depicted lower value of CI (as compared to pure drug) which confirmed their enhanced flowability and compressibility (Table 6). Particle/agglomerates shape and size are commonly recognized as important particulate properties for powder packing and flow. Generally cohesive materials have a HR greater than 1.4 (Cain, 2002). Results of HR depicted in Table 6 revealed that RCD had very poor flowability while low value of HR for all batches of agglomerates depicted significantly higher flowability. These observations were generally attributed to spherical shape and smooth surface of the agglomerates obtained from the process of agglomeration.

3.7. Compression behavior of RCD crystals and agglomerates

An important approach in practice is the focus on the manufacturing of tablets with adequate strength. This ability of a powder or agglomerates formulation to be compressed into tablets with specified strength can be expressed as the formulations' compactibility or packability. As the compression process consists of several stages, it may seem unrealistic to look for one relatively simple formula with few parameters covering the entire compression process. It is, consequently, generally agreed that the mathematical models fit the data in either the initial or the final stage of the densification process. As the density during compression is wavering in

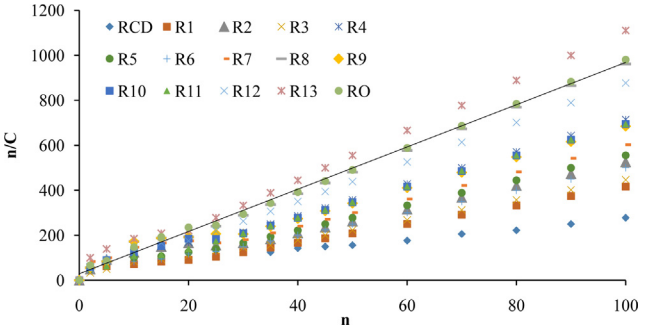

Fig. 11. Kawakita plot of pristine RCD and its agglomerates.

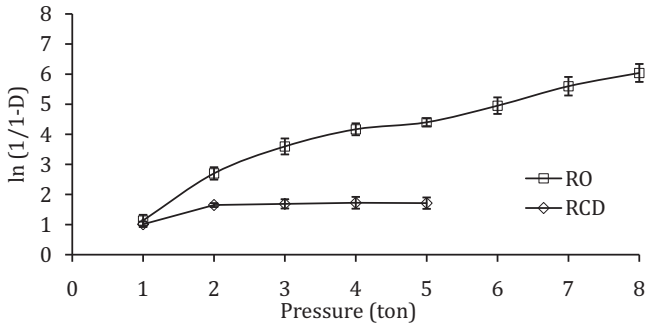

Fig. 12. Heckel plot of pristine RCD and optimized agglomerates.

the tablet, it must be expected that the different stages of the process overlap each other. This creates it challenging or impossible to point out distinct regions where only one type of deformation – plastic, elastic or brittle – is dominating (Sonnergaard, 1999). Attempts have been made to describe the entire compression profile in distinct parts by several equations (Holman, 1991) or with a polynomial with several coefficients (Chen and Malghan, 1994). In order to investigate compression behavior of prepared agglomerates of RCD, Kawakita analysis, Kuno's equation and Heckel analysis were performed.

Kawakita parameters were obtained by linear regression analysis (Fig. 11). The linear region of the Kawakita plot was determined visually, and all the plots were taken between 0–100 tapping. The R^2 values for both RCD and all other batches including RO (indicated by line graph in Fig. 11) were >0.9. The parameter *a* explains the initial porosity at zero pressure which is corresponding to the total portion of reducible volume at maximum pressure. It also describes the relative volume reduction at the maximum number of taps. In case of prepared agglomerates of RCD, value of *a* (<0.2581) was significantly smaller than value of RCD (0.4245), indicating excellent flowability and better packability of agglomerated crystals over RCD. Here, RCD had higher *a* value than RO (1.065), which could be attributed to needle shape structure of primary RCD particles, possessing large amount of voids between them. The less *a* value of RO was due to the smaller size and spherical shape of the particles, which would facilitate efficient packing (Busignies et al., 2012). In other words they were well packed before tapping since tapping does not improve the packing significantly, it only reorganizes the agglomerated particles presumably without changing their shape and size significantly (Barot et al., 2012). The apparent packing velocity obtained by tapping, represented by parameter *1/b*, for the agglomerates was lower than that for the pure drug, since the agglomerates were packed more closely, even without any tapping, as a consequence of their better flowability and packability (Nokhodchi et al., 2007). Mathematically, the parameter *1/b* is equal to the pressure when the value of *C* reaches one-half of the limiting value (Klevan et al., 2010), and for the prepared agglomerates the *1/b* parameter ranges from 2.8068 to 9.4576. The mean particle size of RCD (0.179 mm) was less than RO (0.7312 mm). The *1/b* values for RCD and RO were 17.45 and 3.10, respectively. Thus, RO requires greater force to reduce to one-half of its original volume than RCD, as needle shape crystals get packed with high amount of rearrangement, which requires higher force (Mazel et al., 2011). The larger *b* value of RO (0.322) than RCD (0.0573) implied that comparatively less resisting forces could occur for agglomerated crystals during compression (Joshi et al., 2010). Improved flow properties and compressibility of the agglomerated crystals indicated that they were directly compressible; whereas, the non-agglomerated drug would be predicted to be not directly compressible due to its poor flow properties. In other words, the powders became more resistant to compression at low pressure range opposite to agglomerates. The compression profiles also indicate that smaller particle size of drug tended to reduce the ability of the powders to compress. This may reflect that smaller size materials are less prone to deform.

Furthermore, large values of parameter *K* (>0.9) in Kuno's equation for the agglomerates indicated that the rate of their packing process was much higher than that of the original crystals. These findings suggested that agglomerates flow and pack smoothly from the hopper into the die and that tablets formed from agglomerates attain uniformity in weight (Nokhodchi et al., 2007; Patra et al., 2007).

The Heckel equation is probably the most widely used porosity–pressure function in the field of pharmaceutical sciences. Heckel suggested (Heckel, 1961b) density–pressure relationship during powder compaction in analogous to a first order chemical reaction. Heckel plot constant, *A* is the intercept of the extrapolated linear region of the curve (Fig. 12). Its value is related to the density of the powder after die filling and particle rearrangement in the initial phase of compaction before bond formation. Table 6 shows parameters of Heckel plot. Values of *A* for all the batches of agglomeration were less than pure drug (1.375). This finding suggests that low compression pressure was required to obtain closest packing of the particles, fracturing its texture and densifying the fractured particles (Kawashima, 1984).

Heckel (1961a) argued that the linear part of the curve described the plastic deformation of the material and considered elastic deformation to be negligible. The slope of the linear region of the curve, *k*, provided information of the plasticity of the compressed powder. The higher value of the slope *k* for all the prepared batches indicated more plastic nature of agglomerates than the RCD. The value of slope was also related to the mean yield pressure (Py) of the material (Hersey and Rees, 1971), which measured the material's resistance for deformation. Plastic flow of the particles during compression occurred mainly after rearrangement and fracture (Kawashima et al., 2002). The Heckel yield pressure, Py, represented the compressibility of the powder in region II and varied from 29.239 ton (RCD) to 1.208 ton (R12), i.e. a ~24-fold variation. Since, the Heckel yield pressure is often used as an indication of the plasticity of materials, the agglomerates prepared were soft as compared to RCD, as categorized by Roberts and Rowe (1987).

Yield strength (σ_o) is an indication of tendency of the materials to deform either by plastic flow or fragmentation (Paroren and Juslin, 1983). Low value of yield strength (σ_o) (Table 6) is an indication of low resistance to pressure, good densification and easy compaction (Patra et al., 2007). Heckel also concluded that at low pressures, the curved region of the plot was associated with individual particle movement in the absence of interparticle bonding, and that the transition from curved to linear corresponds with the minimum pressure necessary to form a coherent compact

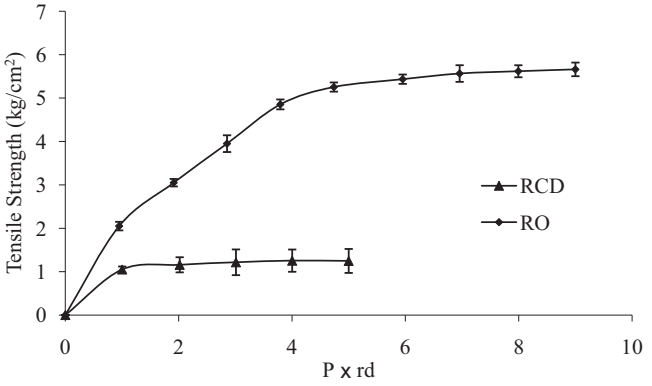

Fig. 13. Leuenberger plot of RCD and RO.

(Heckel, 1961b). In case of agglomerates, effect of PEG 6000 (plastic material) on tableting properties was observed. Densification of this polymer was probably due to plastic deformation (Lin and Chain, 1995). Furthermore, Heckel plot analysis suggested that, agglomerated crystals were fractured easily and new surface of crystals produced might contribute to promote plastic deformation under compression (Kawashima et al., 2003). Therefore, it was concluded that compressibility and tableting behavior of RCD was successfully improved by CCA technique. Furthermore, compreesibility of optimized agglomerated RCD was determined by using Leuenberger analysis.

Leuenberger (1982) derived an equation, which includes one factor for compressibility and the other for compactibility. The inclusion of a compactibility term made this equation, the so-called Leuenberger equation, an attractive tool for investigating powder formulations. Interrelation between these two characteristics can be expressed by the following equation.

$$\sigma_t = \sigma_{t\,\max}(1 - e^{-\gamma P_\rho}) \quad (16)$$

where σ_t is radial CS at certain pressure (kg/cm^2); $\sigma_{t\max}$ is maximum CS (MPa); γ is compression susceptibility ((kg/cm^2)$^{-1}$); P is applied force and ρ is relative density. A non-linear plot (Fig. 13) of tensile strength with respect to product of compaction pressure (P) and relative density (rd) was obtained using statistical software GraphPad Prism 5.03 (GraphPad Software, Inc., USA). The parameter maximum CS ($\sigma_{t\max}$) and compression susceptibility (γ) allows the characterization of different materials (Jetzer et al., 1983). The compression susceptibility for compact prepared from RO indicated that the maximum CS was reached faster at lower pressures of compression as opposed to crystals of RCD. Higher value for $\sigma_{t\max}$ was observed in case of agglomerates than RCD compression. It showed that agglomerates can build a compact with higher strength than RCD. Lower value of γ for RCD crystals demonstrated that maximum tensile strength could be obtained slowly at higher pressure. Low $\sigma_{t\max}$ value for powder showed poor bonding properties. In this regard RCD formulations showed least bonding properties (Table 10).

Table 10
Parameters of Leuenberger equation.

Sample	Compression susceptibility[a], γ ((kg/cm^2)$^{-1}$)	Maximum crushing strength[a], $\sigma_{t\max}$ (kg/cm^2)
RCD	0.0217 ± 0.0073	1.253 ± 0.131
RO	0.0945 ± 0.0102	5.661 ± 0.227

[a] Results are of mean of three observations ±SD.

3.8. Elastic recovery

To investigate the effects of interparticulate friction, elastic recovery measurements were made on prepared compacts. The results of elastic recovery for RCD and agglomerates are given in the Table 6. Elastic recovery of all the prepared agglomerates were very small (<0.82%). Capping/lamination of the original coarse crystals occurred at compression pressures of 4 ton and above. At the same time, the elastic recovery of pure drug was very high (4.45%). When RCD was made into crystal agglomerates by CCA, tableting was possible without the occurrence of capping. Spherically agglomerated crystals of RCD showed significantly improved tabeltability than coarse crystals, because agglomerates fracture the crystals easily under compression, which increases the points of contact among the particles facilitating plastic flow, thereby increasing the contact area and thus new high-energy surfaces appeared because of fracturing, which strongly bonded the particles (Kawashima et al., 2003; Kawashima et al., 1994).

3.9. Tensile strength

The agglomerated crystals, obtained by crystallization in the presence of excipients like HPMC and PEG, possessed superior tensile strength characteristics in comparison to the pure crystals (Table 6). The results showed that the tablets made of untreated RCD particles were prone to capping at lower compression pressures, while the agglomerated crystals were successfully tableted without capping at any compression pressure applied. This was the main reason for higher tensile strength of tablets from agglomerated particles in comparison to the tablets made from the untreated RCD (1.253 kg/cm^2). The maximum tensile strength for RO (5.661 kg/cm^2) was obtained at compression pressure 9 ton.

3.10. Moisture content

The MC of pure drug and agglomerates influenced flowability from the perspective of capillary forces and liquid bridging between the particles. The strength of the cohesive force depends on the surface tension, wetting angle, space between the particles and particle diameter. The same particle characteristics that result in moisture uptake would influence dissolution properties. This parameter was also important for the prediction of the flow behavior of the product in tableting machines or in encapsulation machines during the preparation of pharmaceutical dosage forms. It is worthwhile to note that moisture played a critical role in compression. One of the most common causes of capping in tablets was inadequate moisture in the blend ready for compression. In terms of residual moisture, results of MC of the agglomerated crystals of RCD was found to be less than 1.2% (Table 6), which could attribute to the hygroscopic nature of PEG 6000 that retained moisture, even after drying (Motlekar and Youan, 2008). The data were in compliance with USP requirements for product storage (USP, 1994).

3.11. Fourier transform-infrared (FT-IR) spectroscopy

Infrared (IR) spectral measurements were used for a broad range of applications – from analysis of liquids, gas compositions and solid substances for detailed characterization of their physical state. The compatibility of RCD with polymer was investigated by IR spectroscopy study and the IR spectra of RCD and RO are illustrated in Fig. 14.

One of the fundamental properties of chemical bonds is that they exhibit vibrations at distinct frequencies. The vibrational frequency of a chemical bond is intrinsic to the chemical bond of interest (Jamrogiewicz, 2012). The study of IR spectra of RCD (Fig. 14) demonstrated characteristic absorption bands for

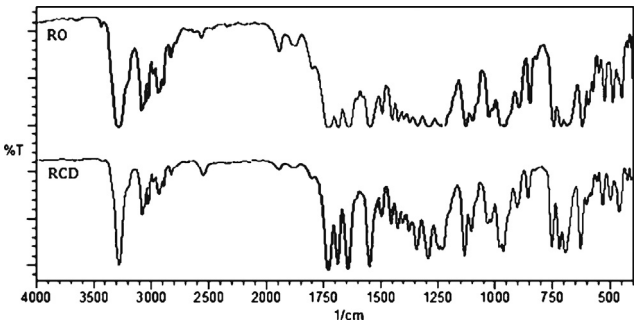

Fig. 14. FT-IR spectra of RCD and RO.

aromatic rings like S—H stretching, C=O stretching, C—O stretching and N—H stretching vibration appeared at 1542, 2554, 1641, 1039 and 3306 cm^{-1}, respectively. Almost identical absorption bands were obtained from FT-IR spectra of optimized agglomerates (RO), but with lower intensity. Thus, the IR study indicated a stable nature of RCD in agglomerated crystals. All the peaks of drug appeared in the spherical agglomerates of RCD, which showed that there was no interaction between drug and excipients utilized.

.

3.12. Differential scanning calorimetry (DSC)

The DSC thermograms of RCD and RO have been demonstrated in Fig. 15. Pure drug showed a sharp endothermic peak at 81.20 °C, with the heat of fusion/enthalpy (ΔH) of 71.3 J/g, corresponding to its melting point. This sharp peak confirmed the purity of the drug substance, with no noticeable impurities present, corresponding to the literature value of 82 °C (Tao et al., 2006). In DSC thermogram of RO, peak corresponding to melting point of RCD was observed at 79.45 °C and it was negligibly broadened. Slightly lower melting point and reduction in ΔH of RO (43.17 J/g) implies the presence of amorphousness in the sample which might be due to weakening as well as disrupting of crystal lattice and order (Bolourtchian et al., 2001). Also, these occurrence may be due to dispersion of crystalline RCD into amorphous polymer i.e. PEG and HPMC, further it was not a sign of pharmaceutical incompatibility (Palanisamy and Khanam, 2011; Das and Rao, 2007). Partial amorphization of crystalline RCD in agglomerates may also be a reason for such phenomena (Modi and Tayade, 2005). In order to evaluate the amorphous/crystalline property quantitatively, the relative ratio of heat of fusion against the original bulk, was defined as crystallinity (Xcr), and it was calculated from the heat of fusion of DSC thermogram. The data revealed that crystallinity of the RO was decreased (crystallinity index, Xcr = 60.54%) than pure crystalline RCD (Xcr = 100%).

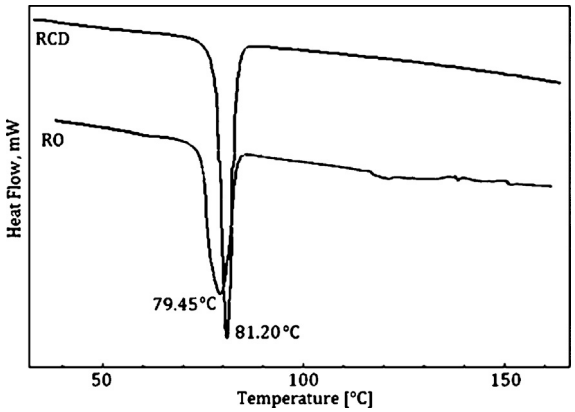

Fig. 15. DSC thermogram of RCD and RO.

3.13. Powder X-ray diffraction (PXRD)

PXRD can be used to screen for the relative crystallinity (RC) of samples (Varlashkin, 2011) which is expressed in terms of relative degree of crystallinity (RDC) or crystallinity index (Naidu et al., 2004). For the determination of degree of crystallinity, a number of X-ray diffraction methods were reported and practiced (Murthy, 2004). Typically PXRD assessed crystallinity from peak height (Terinte et al., 2011) or area (Randall and Rocco, 2010). In the present investigation, RDC was calculated by the following equation:

$$\mathrm{RDC} = I_s / I_r \tag{17}$$

where I_s was peak height of the sample (optimized agglomerated crystals) under investigation and I_r was the peak height at the same angle of the reference (crystalline drug) with the highest intensity. Because crystalline drug was not observed "halo" in the PXRD pattern, the external standard method was reduced to a direct comparison method and therefore, it was assumed that coarse crystalline drug has 100% crystallinity. The RC in percentage was calculated as follows:

$$\mathrm{RC}(\%) = (C_s / C_r) \times 100 \tag{18}$$

where, C_s and C_r are the product of peak height and Kubler Index (is the full width at half-maximum height, FWHM) (Jaboyedoff et al., 2001) of highest intense peak of sample (optimized agglomerated crystals) and reference (crystalline drug), at same angular scale, respectively.

The PXRD pattern of RCD exhibited intense peaks whereas for agglomerated crystals (RO) it exhibited less intense and denser peaks compared to pristine RCD (Fig. 16). The PXRD pattern of RCD showed its characteristic peaks with decreased percent relative intensity at°2θ of 18.04, 20.22, 25.69, 25.13, 23.56, 17.10, 41.71 and 31.34, respectively. In case of RO, PXRD pattern in the°2θ range of

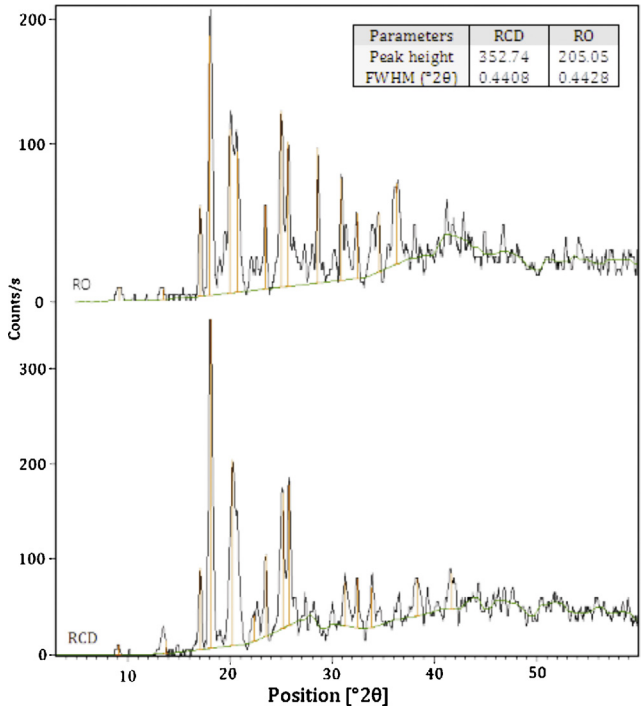

Fig. 16. PXRD patterns of RCD and RO.

5–50 illustrated characteristic diffraction peaks of RCD. Intensities of characteristic peaks of drug were decreased in RO, which may be due to differences in the crystallinity of the drug and agglomerates (Jbilou et al., 1999), indicating reduction in crystallinity or partial amorphization of the drug in its agglomerated form (Rasenack and Müller, 2002b). In RC determinations, the PXRD patterns of RCD and RO were clearly different in peak intensity. The maximum intensity of the RCD peaks was observed at 18.04 °2θ and in case of RO at 17.98 °2θ. The calculated RDC and RC value for RO was 0.58 and 57.86%, respectively, further indicating the reduction in crystallinity of drug when formulated as spherical crystal agglomerates. Also it was found that the particles crystallized in the presence of excipients did not undergo structural modifications. As depicted in the Fig. 16, most of PXRD peaks of the agglomerates were consistent with the pattern of pure drug crystals, indicating that there was no structural changes or drug-excipients incompatibility detected after recrystallization (Gupta et al., 2007).

PXRD pattern of agglomerated crystals illustrated the presence of numerous reflections that match those in crystalline RCD superimposed on a broad diffusive scattered pattern with reduced peak height caused by agglomerated crystals (Table 11). This indicated that the crystalline form of RCD determined by PXRD analysis persisted in the agglomerated crystals. However, these reflections were significantly broadened relative to the crystalline pattern. Line profile analysis, a diffraction technique was used to obtain microstructural information of the pure RCD and agglomerates (Table 11). In a PXRD, a crystalline material without any lattice strain and consisting of larger particle size, showed sharp narrow diffraction peaks (Padrela et al., 2012) and the amorphous component exhibited a very broad peak (halo) (Hauk, 2000). The broadening observed in the pattern of the agglomerated RCD provided an initial indication of reduction in crystallinity and contribution of agglomerates (Vogt and Williams, 2010; Langford and Wilson, 1978; Park et al., 2010). This was a good assumption in the present case because the crystalline RCD showed the presence of large crystals by optical microscopy and also, agglomerated crystals obtained by CCA lost long-range crystalline order, without complete transition to an amorphous form (Deng et al., 2008).

3.14. Determination of residual solvent

Residual solvents are critical impurities in excipients, drug substances and ultimately drug products, because they may cause toxicity and safety issues, and affect physicochemical properties of drug substances and drug products (Cheng et al., 2010). In order to control residual solvent contents in drug substances, products and excipients, ICH Q3C guideline provides specific criteria for Class 1 solvents (5) – known or suspected human carcinogens or environmental hazards, Class 2 solvents (26) – suspected of other significant but reversible toxicities, and Class 3 (28) solvents – low toxic potential to man (ICH, 2011). Generally, the solvents were not completely removed by practical manufacturing techniques. Hence, the solvent may sometimes be a critical parameter in the process. The general procedure of European Pharmacopoeia for residual solvent determination in pharmaceutical products included analysis of many solvents by GC (European Pharmacopoeia, 2005).

A GC-HS chromatogram of standard solution and RCD agglomerates is shown in Fig. 17. The detector voltage (y-axis) was plotted as a function of time (x-axis). The identity of each peak was determined by injecting samples and noting their retention times. After injecting standard solution of DCM (1000 ppm), a peak corresponds to a DCM content that appeared at retention time of 1.03 min. A residual solvent peak of optimized RCD agglomerates was also observed at the same retention time as that of standard (1.03 min) with extremely low intensity. It depicted that most of the solvents

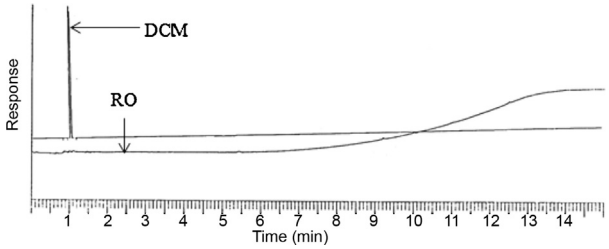

Fig. 17. GC-HS chromatogram for determination of DCM in RCD agglomerates.

had evaporated and very small amount of solvent was retained in the agglomerates. Further, the amount of DCM was determined by area covered by peak at same retention time and it was found to be 18.46 ppm. The "permitted daily exposure" (PDE) for DCM was defined by ICH as 600 ppm (ICH, 2011). Hence, it revealed that DCM was entrapped in agglomerates at insignificant extent and that may not produce toxicity in humans.

3.15. Scanning electron microscopy

An examination of the SEMs, confirmed that the pristine RCD (Fig. 18(a)) was significantly smaller in particle size and blade or plate shaped elongated crystals with fines which hindered the flowability and compressibility. Improved flowability of RCD agglomerates was mainly because of good sphericity of modified crystals obtained (Fig. 18(b)) by CCA. Similar results were obtained in other studies using CCA procedures for other drugs (Raval et al., 2013; Jadhav et al., 2007; Paradkar et al., 2002). SEMs of the untreated RCD (Fig. 18(a)) show no evidence of porosity in the untreated RCD crystals, whereas the crystallized agglomerated particles indicated clear evidence of porosity. RCD crystallized and agglomerated in the presence of HPMC and PEG (Fig. 18(b)) were spherical in shape with smooth surface appearance which promotes flowability.

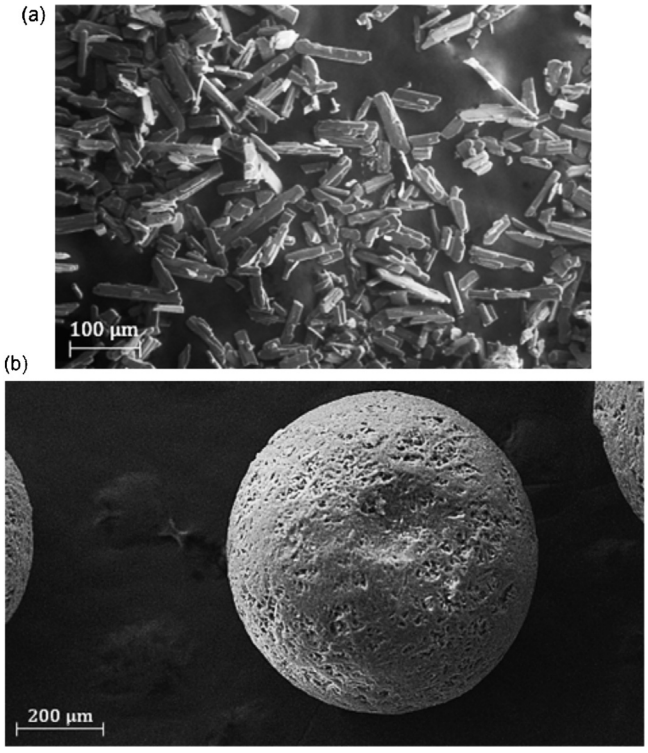

Fig. 18. SEM micrographs of pristine (a) and optimized agglomerates (b) of RCD.

Table 11
Line profile of PXRD pattern of RCD and RO.

Sr. no.	RCD			RO		
	Position (°2θ)	Height (cps)[a]	FWHM[b] (°2θ)	Position (°2θ)	Height (cps)	FWHM (°2θ)
1	17.10	86.71	0.3444	17.07	71.5	0.3693
2	18.04	352.74	0.4408	17.98	205.05	0.4428
3	20.22	196.08	0.2952	20.72	110.94	0.3936
4	23.56	86.16	0.2952	23.43	65.67	0.3444
5	25.13	141.9	0.3936	24.97	139.24	0.3936
6	25.69	147.64	0.2952	25.65	114.24	0.3954
7	31.34	45.29	0.4594	32.44	44.85	0.5904
8	41.71	37.32	0.9600	36.32	63.3	0.7872

[a] cps, counts per second.
[b] FWHM, full width at half-maximum height.

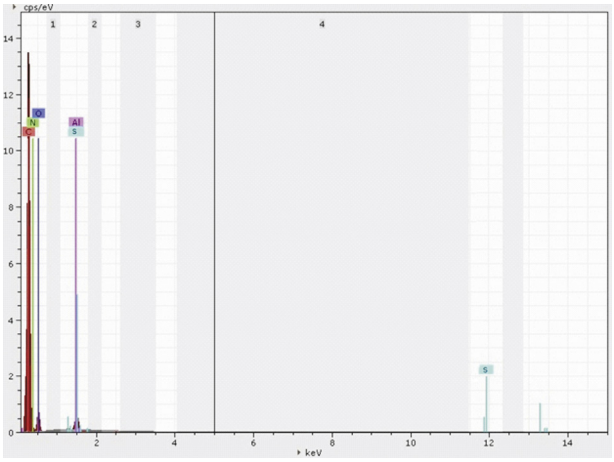

Fig. 19. Elementary analysis of RCD agglomerates.

These agglomerates were better distinguished by using secondary electrons (Fig. 19) and due to the existence of nitrogen in the RCD molecule, agglomerates were recorded with lighter hue than that of the matrix (Papadimitriou et al., 2012). This procedure appeared as added advantage of SEM for studying spherical agglomerates, since many drug molecules have detectable heavy elements. Elementary analysis of these agglomerates revealed that apart from nitrogen, RCD molecule also contains components like oxygen, carbon and sulfur which may be attributed to RCD (Fig. 19). Elementary analysis of RCD agglomerates also showed the presence of aluminum and it may be because of impurities present mainly in excipients like talc and, sometimes, to a certain extent in drug.

3.16. Dissolution of RCD agglomerates

Dissolution of optimized agglomerates (RO) and pure RCD in previously optimized media was performed using USP type II apparatus (Garala et al., 2013). The aliquots of dissolution were subjected to analysis by HPLC method developed (Kevin et al., 2012). Dissolution profile of RO showed 97.35% drug release within 90 min while pure drug showed less than 83% drug release (Fig. 20). Drug release profile showed improvement in percentage drug dissolved from agglomerates after 5 min ($\%DP_{5\,min} = 79.36$) compared to pure drug ($\%DP_{5\,min} = 69.35$). The reason for this improved dissolution was linked to the better wettability of the spherically agglomerated crystals. Addition of the hydrophilic polymer might have contributed in improved dissolution rate. The increase of the dissolution rate of agglomerates was also attributed to the better uniformity of agglomerates and reduced crystallinity (Bhole and Patil, 2009).

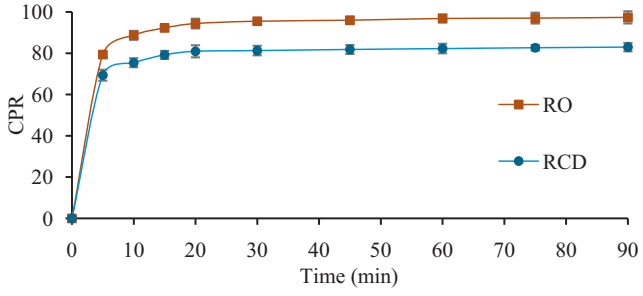

Fig. 20. Dissolution profile of RCD and RO.

4. Conclusions

CCA technique could be successfully employed as an alternative to conventional wet granulation. This study has shown that it is possible to quantify differences between pristine RCD crystals and agglomerated RCD by a quick and simple screening method. The RCD agglomerates were successfully prepared by application of Box–Behnken experimental design and characterized by 21 different variables. In combination with multivariate evaluation methods such as PCA, this approach was successful in distinguishing, quantifying and predicting the most influencing variables of agglomerates. Based on these findings, the present approach serves as the first step toward a 'formulation tool' for optimizing various agglomerate properties with respect to formulate directly compressible tablets. Optimized agglomerates of RCD consisting of 4.04% PEG 6000, 1% talc, 1% HPMC E50LV and 1.5% PVA which was prepared at room temperature with phase ratio (DCM: water) of 0.065 and stirring rate of 874 rpm. In addition, agglomerates of RCD were obtained with excellent physico-mechanical properties. Agglomerates possessed increased particle size, sphericity and surface smoothness which resulted in excellent flow and packability due to reduced interparticulate friction. The dissolution study of the agglomerates showed slight increase in the rate of drug release compared to pure RCD. The systematic statistical approach enables to obtain ready-to-compress agglomerates of active pharmaceutical ingredients by omitting time-consuming conventional wet granulation methods using novel CCA technique.

References

Armstrong, N.A., Haines-Nutt, R.F., 1974. Elastic recovery and surface area changes in compacted powder systems. Powder Technol. 9, 287–290.
Barot, B.S., Parejiya, P.B., Patel, T.M., Parikh, R.K., Gohel, M.C., 2012. Compactibility improvement of metformin hydrochloride by crystallization technique. Adv. Powder Tech. 23, 814–823.
Batt, D., Garala, K., 2012. Preparation and evaluation of inclusion complexes of diacerein with β-cyclodextrin and hydroxypropyl β-cyclodextrin. J. Incl. Phenom. Macro. Chem., http://dx.doi.org/10.1007/s10847-012-0268-8.

Bhole, P.G., Patil, V.R., 2009. Enhancement of water solubility of Felodipine by preparing solid dispersion using poly-ethylene glycol 6000 and poly-alcohol. Asian J. Pharm. 3, 240–244.
Bolourtchian, N., Nokhodchi, A., Dinarvand, R., 2001. The effect of solvent and crystallization condition on habit modification of carbamazepine. DARU J. Pharm. Sci. 9, 12–22.
Busignies, V., Mazel, V., Diarra, H., Tchoreloff, P., 2012. Prediction of the compressibility of complex mixtures of pharmaceutical powders. Int. J. Pharm. 436, 862–868.
Cain, J., 2002. An alternative technique for determining ANSI/CEMA standard 550 flowability ratings for granular materials. Powder Hand Proc. 14, 218–220.
Carr, R.L., 1965. Evaluating flow properties of solids. Chem. Eng. 72, 163–168.
Cattell, R.B., 1966. The scree test for the number of factors. J. Multiv. Behav. Res. 1, 245–276.
Chaulang, G., Patil, K., Ghodke, D., Khan, S., 2008. Preparation and characterization of solid dispersion tablet of Furosemide with crospovidone. Res. J. Pharm. Technol. 1, 386–389.
Chavda, V., Maheshwari, R., 2008. Tailoring of ketoprofen particle morphology via novel crystallocoaglomeration technique to obtain direct compressible material. Asian J. Pharm. 2, 61–67.
Chen, W., Malghan, S.G., 1994. Investigation of compaction equations for powders. Powder Technol. 81, 75–81.
Chen, X.J., Miao, W., Liu, Y., Shen, Y.F., Feng, W.S., Yu, T., Yu, Y.H., 2006. Microcalorimetry as a possible tool for phylogenetic studies of tetrahymena. J. Therm. Anal. Cal. 84, 429–433.
Chow, A.H.L., Leung, M.W.M., 1996. A study of the mechanisms of wet spherical agglomeration of pharmaceutical powders. Drug Dev. Ind. Pharm. 4, 357–371.
Cooper, V.B., Pearce, G.E., Petts, C.R., 2003. Quantification of crystalline forms in active pharmaceutical ingredient and tablets by X-ray powder diffraction. J. Pharm. Pharmacol. 55, 1323–1329.
Craik, D.J., Miller, B.F., 1958. The flow properties of powders under humid conditions. J. Pharm. Pharmacol. 10, 136–144.
Cutrignelli, A., Lopedota, A., Trapani, A., Boghetich, G., Francoa, M., Denora, N., Laquintana, V., Trapani, G., 2008. Relationship between dissolution efficiency of Oxazepam/carrier blends and drug and carrier molecular descriptors using multivariate regression analysis. Int. J. Pharm. 358, 60–68.
Dai, X., Moffat, J.G., Wood, J., Reading, M., 2012. Thermal scanning probe microscopy in the development of pharmaceuticals. Adv. Drug Del. Rev. 64, 449–460.
Das, M.K., Rao, K.R., 2007. Microencapsulation of zidovudine by double emulsion solvent diffusion technique using ethyl cellulose. Indian J. Pharm. Sci. 69, 244–250.
Deng, Z., Xu, S., Li, S., 2008. Understanding a relaxation behavior in a nanoparticle suspension for drug delivery applications. Int. J. Pharm. 351, 236–243.
Esbensen, K., 2006. Multivariate Analysis in Practice, fifth ed. Camo ASA, Trondheim.
Council of Europe, 2005. European Pharmacopoeia, fifth ed. Directorate for the Quality of Medicines of the Council of Europe, Strasbourg.
Faria, A.F., Marcellos, L.F., Vasconcelos, J.P., de Souza, M.V.N., Júnior, A.L.S., do Carmo, W.R., Diniza, R., de Oliveira, M.L.A., 2011. Ethambutol Analysis by copper complexation in pharmaceutical formulations: spectrophotometry and crystal structure. J. Braz. Chem. Soc. 22, 867–874.
Fell, J.T., Newton, J.M., 1970. Determination of tablet strength by the diametral compression test. J. Pharm. Sci. 59, 688–691.
Ganesan, V., Rosentrater, K.A., Muthukumarappan, K., 2008. Flowability and handling characteristics of bulk solids and powders – a review with implications for DDGS. Biosyst. Eng. 101, 425–435.
Ganjian, F., Cutie, A.J., Jochsaberger, T., 1980. In vitro adsorption studies of cimetidine. J. Pharm. Sci. 69, 352–353.
Garala, K., Patel, J., Dhingani, A., Raval, M., Dharamsi, A., 2013. Overcoming limitations in dissolution testing of poorly water soluble racecadotril. Inventi. Rapid: Pharm Tech. 2013, 1–4.
Gokonda, S.R., Hileman, G.A., Upadrastha, S.M., 1994. Development of matrix controlled release beads by extrusion–spheronization techniques technology using a statistical screening design. Drug Dev. Ind. Pharm. 20, 279–292.
Gordonx, M.S., Chowhan, Z.T., 1990. Manipulation of naproxen particle morphology via the spherical crystallization technique to achieve a directly compressible raw material. Drug Dev. Ind. Pharm. 16, 1279–1290.
Gupta, V.R., Mutalik, S., Patel, M.M., Jani, G.K., 2007. Spherical crystals of celecoxib to improve solubility, dissolution rate and micromeritic properties. Acta Pharm. 57, 173–184.
Hauk, V., 2000. Structural and residual stress analysis by X-ray diffraction on polymeric materials and composites, JCPDS-International Centre for Diffraction Data. Adv. X-ray Anal. 42, 540–554.
Hausner, H.H., 1967. Friction conditions in a mass of metal powder. Int. J. Powder Metall. 3, 7–13.
Haware, R.V., Tho, I., Bauer-Brandl, A., 2009. Multivariate analysis of relationships between material properties, process parameters and tablet tensile strength for a-lactose monohydrates. Eur. J. Pharm. Biopharm. 73, 424–431.
Heckel, R.W., 1961a. Density–pressure relationships in powder compaction. Trans. Metall. Soc. AIME 221, 671–675.
Heckel, R.W., 1961b. An analysis of powder compaction phenomena. Trans. Metall. Soc. AIME 221, 1001–1008.
Hersey, J.A., Rees, J.E., 1971. Deformation of particles during briquetting. Nat. Phys. Sci. 230, 96.
Holman, L.E., 1991. The compaction behaviour of particulate materials: an elucidation based on percolation theory. Powder Technol. 66, 265.
Hu, R., Zhu, J., Chen, G., Sun, Y., Mei, K., Li, S., 2006. Preparation of sustained-release simvastatin microspheres by the spherical crystallization technique. AAPS PharmSciTech. 1 (1), 47–52.
ICH Q3C(R5), Impurities: Guideline for residual solvents. February 2011.**.
Jaboyedoff, M., Bussy, F., Kubler, B., Thelin, P., 2001. Illite "crystallinity" revisited. Clay. Clay Miner. 49, 156–167.
Jadhav, N., Pawar, A., Paradkar, A., 2007. Design and evaluation of deformable talc agglomerates prepared by crystallo-coagglomeration technique for generating heterogeneous matrix. AAPS PharmSciTech. 8, E59.
Jadhav, N., Pawar, A., Paradkar, A., 2010. Effect of drug content and agglomerate size on tabletability and drug release characteristics of bromhexine hydrochloride-talc agglomerates prepared by crystallo-co-agglomeration. Acta Pharm. 60, 25–38.
Jamrogiewicz, M., 2012. Application of the near-infrared spectroscopy in the pharmaceutical technology. J. Pharm. Biomed. Anal. 66, 1–10.
Jarosz, P.J., Parrott, E.L., 1983. Comparison of granule strength and tablet tensile strength. J. Pharm. Sci. 72, 530–535.
Jbilou, M., Ettabia, A., Guyot-Hermann, A., Guyot, J.C., 1999. Ibuprofen agglomerates preparation by phase separation. Drug Dev. Ind. Pharm. 25, 297–305.
Jetzer, W., Leuenberger, H., Sucker, H., 1983. The compressibility and compactibility of pharmaceutical powders. Pharm. Technol. 7, 33–39.
Johansen, A., Schaefer, T., Kristensen, H.G., 1999. Evaluation of melt agglomeration properties of polyethylene glycols using a mixer torque rheometer. Int. J. Pharm. 183, 155–164.
Joshi, A., Shah, S.P., Mishra, A.N., 2003. Preparation and evaluation of directly compressible form of rifampicin and ibuprofen. Ind. J. Pharm. Sci. 65, 232–238.
Joshi, A.B., Patel, S., Kaushal, A.M., Bansal, A.K., 2010. Compaction studies of alternate solid forms of celecoxib. Adv. Powder Technol. 21, 452–460.
Jun, H.K., Dong, H.O., Yu-Kyoung, O., Chul, S.Y., Han-Gon, C., 2012. Effects of solid carriers on the crystalline properties, dissolution and bioavailability of flurbiprofen in solid self-nanoemulsifying drug delivery system (solid SNEDDS). Eur. J. Pharm. Sci. 80, 289–297.
Kadam, S.S., Mahadik, K.R., Paradkar, A.R., 1997. A process for making agglomerates for use as or in a drug delivery system. Indian Patent 183036.
Kaiser, H.F., 1960. The application of electronic computers to factor analysis. Educ. Psychol. Meas. 20, 141–151.
Kawakita, K., Tsutsumi, Y., 1966. A comparison of equations for powder compression. Bull. Chem. Soc. Jap. 39, 1364–1368.
Kawashima, Y., 1984. Development of spherical crystallization technique and its application to pharmaceutical systems. Arch. Pharm. Res. 7, 145–151.
Kawashima, Y., Lin, S.Y., Naito, M., Takenama, H., 1982a. Direct agglomeration of sodium theophylline crystals produced by salting out in liquid. Chem. Pharm. Bull. 30, 1837–1843.
Kawashima, Y., Okumura, M., Takenama, H., 1982b. Spherical crystallization: direct spherical agglomeration of salicylic acid during crystallization. Science 216, 1127–1128.
Kawashima, Y., Okumura, M., Takenaka, H., 1984. The effects of temperature on the spherical crystallization of salicylic acid. Powder Technol. 39, 41–47.
Kawashima, Y., Handa, T., Hirofumi, T., Okumura, M., 1986a. Effects of polyethylene glycol on size of agglomerated crystals of phenytoin prepared by the spherical crystallization technique. Chem. Pharm. Bull. 34, 3403–3407.
Kawashima, Y., Handa, T., Tekeuchi, H., Okumura, M., Katou, H., Nagata, O., 1986b. Crystal modification of phenytoin with polyethylene glycol for improving mechanical strength, dissolution rate and bioavailability by spherical crystallization technique. Chem. Pharm. Bull. 34, 3376–3383.
Kawashima, Y., Cui, F., Takeuchi, H., Niwa, T., Hino, T., Kiuchi, K., 1994. Improvements in flowability and compressibility of pharmaceutical crystals for direct tabletting by spherical crystallization with a two solvent system. Powder Technol. 78, 151–157.
Kawashima, Y., Imai, M., Takeuchi, H., Yamamoto, H., Kazunori Kamiya, K., 2002. Development of agglomerated crystals of ascorbic acid by the spherical crystallization technique for direct tableting, and evaluation of their compactibilities. KONA 20, 251–262.
Kawashima, Y., Imai, M., Takeuchi, H., Yamamoto, H., Kamiya, K., 2003. Development of agglomerated crystals of Ascorbic acid by the spherical crystallization techniques. Powder Technol. 130, 283–289.
Kevin, G., Patel, J., Dhingani, A., Raval, M., Dharamsi, A., 2012. Development and validation of a rapid and sensitive HPLC method for estimation of Racecadotril. Invent. Rapid: Pharm Anal. Qual. Assurance 2013, 1–5.
Klevan, I., Nordström, J., Tho, I., Alderborn, G., 2010. A statistical approach to evaluate the potential use of compression parameters for classification of pharmaceutical powder materials. Eur. J. Pharm. Biopharm. 75, 425–435.
Kubista, M., Sjögreen, B., Forootan, A., Sindelka, R., Jonák, J., Andrade, J.M., 2007. Real-time PCR gene expression profiling. Eur. Pharm. Rev. 1, 56–60.
Kumar, S., Chawla, G., Bansal, A.K., 2008. Spherical crystallization of mebendazole to improve processability. Pharm. Dev. Tech. 13, 559–568.
Kuno, H., 1979. In: Jimbo, G., et al. (Eds.), Funtai (Powder Theory and Application). Maruzen, Tokyo, p. 342.
Langford, J.I., Wilson, A.J.C., 1978. Scherrer after sixty years: a survey and some new results in the determination of crystallite size. J. Appl. Cryst. 11, 102–113.
Leonard, S.T., Droege, M., 2008. The uses and benefits of cluster analysis in pharmacy research. Res. Soc. Admin. Phar. 4, 1–11.
Leuenberger, H., 1982. The compressibility and compactibility of powder systems. Int. J. Pharm. 12, 41–55.
Lin, C.W., Chain, T.M., 1995. Compression behavior and tensile strength of heat-treated polyethylene glycols. Int. J. Pharm. 118, 169–179.

Lin, K., Peck, G.E., 1995. Development of agglomerated talc. I. Evaluation of fluidized bed granulation parameters on the physical properties of agglomerated talc. Drug Dev. Ind. Pharm. 21, 159–173.
Liu, L.X., Marziano, I., Bentham, A.C., Litster, J.D., White, E.T., Howes, T., 2008. Effect of particle properties on the flowability of ibuprofen powders. Int. J. Pharm. 362, 109–117.
Maghsoodi, M., Hassan-Zadeh, D., Barzegar-Jalali, M., Nokhodchi, A., Martin, G., 2007. Improved Compaction and packing properties of naproxen agglomerated crystals obtained by spherical crystallization technique. Drug Dev. Ind. Pharm. 33, 1216–1224.
Maghsoodi, M., Taghizadeh, O., Martin, G.P., Nokhodchi, A., 2008. Particle design of naproxen-disintegrant agglomerates for direct compression by a crystallo-co-agglomeration technique. Int. J. Pharm. 351, 45–54.
Mahmoodi, F., Alderborn, G., Frenning, G., 2010. Effect of lubrication on the distribution of force between spherical agglomerates during compression. Powder Technol. 198, 69–74.
Mallick, S., Pradhan, S.K., Chandran, M., Acharya, M., Digdarsini, T., Mohapatra, R., 2011. Study of particle rearrangement, compression behavior and dissolution properties after melt dispersion of ibuprofen, avicel and aerosil. Res. PharmaSci. 1, 1–10.
Martin, A., Swarbrick, J., Cammarata, A., 1991. Physical Pharmacy: Physical Chemical Principles in the Pharmaceutical Sciences. Varghese Publishing House, Bombay, India.
Mashru, R., Sutariya, V., Sankalia, M., Sankalia, J., 2005. Transbuccal delivery of lamotrigine across porcine buccal mucosa: in vitro determination of routes of buccal transport. J. Pharm. Pharmaceut. Sci. 8, 54–62.
Maurya, D.P., Sultana, Y., Aqil, M., Panda, B.P., Ali, A., 2011. Formulation and optimization of alkaline extracted ispaghula husk microscopic reservoirs of isoniazid by box-behnken statistical design. J. Disper. Sci. Technol. 32, 424–432.
Mazel, V., Busignies, V., Duca, S., Leclerc, B., Tchoreloff, P., 2011. Original predictive approach to the compressibility of pharmaceutical powder mixtures based on the Kawakita equation. Int. J. Pharm. 410, 92–98.
Modi, A., Tayade, P., 2005. Enhancement of dissolution profile by solid dispersion (kneading) technique. AAPS PharmSciTech. 7, E1–E6.
Morishima, K., Kawashima, Y., Takeuchi, H., Niwa, T., Hino, T., 1993. Micromeritic characteristics and agglomeration mechanisms in the spherical crystallization of bucillamine by the spherical agglomeration and the emulsion solvent diffusion methods. Powder Technol. 76, 57–64.
Motlekar, N., Youan, B., 2008. Optimization of experimental parameters for the production of LMWH-loaded polymeric microspheres. Drug Design Dev. Ther. 2, 39–47.
Murthy, N.S., 2004. Recent developments in polymer characterization using X-ray diffraction". Rigaku J. 21, 15–24.
Naidu, N.B., Choudary, K.P.R., Murthy, K.V.R., Satyanarana, V., Hayman, A.R., Becket, G., 2004. Physicochemical characterization and dissolution properties of meloxicam–cyclodextrin binary systems. J. Pharma. Biomed. Anal. 35, 75–86.
Niwa, T., Nakanishi, Y., Danjo, K., 2010. One-step preparation of pharmaceutical nanocrystals using ultra cryo-milling technique in liquid nitrogen. Eur. J. Pharm. Sci. 41, 78–85.
Nokhodchi, A., Maghsoodi, M., Hassan-Zadeh, D., Barzegar-Jalali, M., 2007. Preparation of agglomerated crystals for improving flowability and compactibility of poorly flowable and compactible drugs and excipients. Powder Technol. 175, 73–81.
Padrela, L., de Azevedo, E.G., Velaga, S.P., 2012. Powder X-ray diffraction method for the quantification of cocrystals in the crystallization mixture. Drug Dev. Ind. Pharm. 38, 923–929.
Palanisamy, M., Khanam, J., 2011. Cellulose-based matrix microspheres of Prednisolone inclusion complex: preparation and characterization. AAPS PharmSciTech. 12, 388–400.
Papadimitriou, S.A., Barmpalexis, P., Karavas, E., Bikiaris, D.N., 2012. Optimizing the ability of PVP/PEG mixtures to be used as appropriate carriers for the preparation of drug solid dispersions by melt mixing technique using artificial neural networks. I. Eur. J. Pharm. Biopharm. 82, 175–186.
Paradkar, A.R., Pawar, A.P., Chordiya, J.K., Patil, V.B., Ketkar, A.R., 2002. Spherical crystallization of celecoxib. Drug Dev. Ind. Pharm. 28, 1213–1220.
Paradkar, A.R., Maheshwari, M., Ketkar, A.R., Chauhan, B., 2003. Preparation and evaluation of ibuprofen beads by melt solidification technique. Int. J. Pharm. 255, 33–42.
Paradkar, A.R., Pawar, A.P., Jadhav, N.R., 2010. Crystallo-co-agglomeration: a novel particle engineering technique. Asian J. Pharm. 4, 4–10.
Park, S., Baker, J.O., Himmel, M.E., Parilla, P.A., Johnson, D.K., 2010. Cellulose crystallinity index: measurement techniques and their impact on interpreting cellulase performance. Biotechnol. Biofuel. 3, 1–10.
Paroren, P., Juslin, M., 1983. Compressional characteristics of four starches. J. Pharm. Pharmacol. 35, 627–635.
Patra, N., Singh, S.P., Hamd, P., Vimladevi, M., 2007. A sysyematic study on micromeritic properties and consolidation behavior of the terminaliya Arjuna bark powder for processing into tablet dosage from. Int. J. Pharma. Excip. 6, 6–7.
Pattnaik, S., Swain, K., Bindhani, A., Mallick, S., 2011. Influence of chemical permeation enhancers on transdermal permeation of alfuzosin: an investigation using response surface modeling. Drug Dev. Ind. Pharm. 37, 465–474.
Pawar, A., Paradkar, A., Kadam, S., Mahadik, K., 2004a. Agglomeration of Ibuprofen with talc by novel crystallo-co-agglomeration technique. AAPS PharmSciTech. 5, E55.
Pawar, A., Paradkar, A., Kadam, S., Mahadik, K., 2004b. Crystallo-coagglomeration: a novel process to obtain ibuprofen-paracetamol agglomerates. AAPS PharmSciTech. 5, E44.
Pearson, K., 1901. On lines and planes of closest fit to systems of points in space. Philos. Mag. Ser. 6, 559–572.
Pilpel, N., 1964. The flow properties of magnesia. J. Pharm. Pharmacol. 16, 705–716.
Pingali, K.C., Saranteas, K., Foroughi, R., Muzzio, F.J., 2008. Practical methods for improving flow properties of active pharmaceutical ingredients. Drug Dev. Ind. Pharm. 35 (12), 1460–1469.
Rajalahti, T., Kvalheim, O.M., 2011. Multivariate data analysis in pharmaceutics: a tutorial review. Int. J. Pharm. 417, 280–290.
Randall, C.S., Rocco, W.L., 2010. XRD in Pharmaceutical analysis: a versatile tool for problem-solving. Am. Pharm. Rev., 52–59.
Rasenack, N., Müller, B.W., 2002a. Crystal habit and tableting behavior. Int. J. Pharm. 244, 45–57.
Rasenack, N., Müller, B.W., 2002b. Properties of ibuprofen crystallized under various conditions: a comparative study. Drug Dev. Ind. Pharm. 28, 1077–1089.
Raval, M.K., Sorathiya, K.R., Chauhan, N.P., Patel, J.M., Parikh, R.K., Sheth, N.R., 2013. Influence of polymers/excipients on development of agglomerated crystals of secnidazole by crystallo-co-agglomeration technique to improve processability. Drug Dev. Ind. Pharm. 39 (3), 437–446.
Ribardiere, P., Tchoreloff, G., Puisieux, F., 1996. Modification of ketoprofen bead structure produced by the spherical crystallization technique with a two-solvent system. Int. J. Pharm. 144, 195–207.
Ringer, M., 2008. What is principal component analysis? Nat. Biotech. 26, 303–304.
Roberts, R.J., Rowe, R.C., 1987. The compaction of pharmaceutical and other model materials – a pragmatic approach. Chem. Eng. Sci. 42, 903–911.
Rogers, T.L., Wallick, D., 2012. Reviewing the use of ethylcellulose, methylcellulose and hypromellose in microencapsulation. Part 3: Applications for microcapsules. Drug Dev. Ind. Pharm. 38 (5), 521–539.
Roy, P., Shahiwala, A., 2009. Statistical optimization of ranitidine HCl floating pulsatile delivery system for chronotherapy of nocturnal acid breakthrough. Eur. J. Pharm. Sci. 37, 363–369.
Sarfaraz, M., Khan, K., Doddayya, H., Reddy, S., Udupi, R., 2011. Particle design of aceclofenac-disintegrant agglomerates for direct compression by crystallo-co-agglomeration technique. Asian J. Pharm. Tech. 1, 40–48.
Schwartz, J.C., Lecomte, J.M., 2009. Form of administration of racecadotril. US Patent 20090186084, A1.
Shah, T.J., Amin, A.F., Parikh, J.R., Parikh, R.H., 2007. Process optimization and characterization of poloxamer solid dispersions of a poorly water-soluble drug. AAPS PharmSciTech. 8, E1–E7.
Singh, B., Dahiya, M., Saharan, V., Ahuja, N., 2005a. Optimizing drug delivery systems using systematic "design of experiments." Part II: retrospect and prospects. Crit. Rev. Ther. Drug Carrier Syst. 22, 215–294.
Singh, B., Kumar, R., Ahuja, N., 2005b. Optimizing drug delivery systems using systematic "design of experiments." Part I: fundamental aspects. Crit. Rev. Ther. Drug Carrier Syst. 22, 27–105.
Singh, S.K., Verma, P.R.P., Razdan, B., 2010. Development and characterization of a lovastatin loaded self-microemulsifying drug delivery system. Pharm. Dev. Tech. 15, 469–483.
Sobrinho, J.L.S., Lima, L.N.A., Perrelli, D.C., da Silva, J.L., de Medeiros, F.P.M., La Roca Soares, M.F., Rolim Neto, P.J., 2008. Development and in vitro evaluation of tablets based on the antichagasic benznidazole. Braz. J. Pharm. Sci. 44, 383–389.
Sonnergaard, J.M., 1999. A critical evaluation of the Heckel equation. Int. J. Pharm. 193, 63–71.
Sprockel, O.L., Sen, M., Shivanand, P., Prapaitrakul, W., 1997. A melt extrusion process for manufacturing matrix drug delivery systems. Int. J. Pharm. 155, 191–199.
Srinivasan, S., Rengarajan, B., Prabagar, B., Pritam, T., Chul, S.Y., Bong, K.Y., 2011. Solid self-nanoemulsifying drug delivery system (S-SNEDDS) containing phosphatidylcholine for enhanced bioavailability of highly lipophilic bioactive Carotenoid lutein. Eur. J. Pharm. Sci. 79, 250–257.
Stodghill, S.P., 2010. Thermal analysis – a review of techniques and applications in the pharmaceutical sciences. Am. Pharm. Rev., 29–36.
Tao, Y.-T., Zhan, D., Zhang, K.-L., 2006. Kinetics of thermal decomposition of racecadotril in air. Acta Chim. Sinica 64, 435–438.
Terinte, N., Ibbett, R., Schuster, K.C., 2011. Overview on native cellulose and microcrystalline cellulose structure studied by X-ray diffraction (WAXD): comparison between measurement techniques. Lenzinger Berichte. 89, 118–131.
Teychene, S., Sicre, N., Biscans, B., 2010. Is spherical crystallization without additives possible? Chem. Eng. Res. Des. 88, 1631–1638.
Thati, J., Rasmuson, A., 2011. On the mechanism of formation of spherical agglomerates. Eur. J. Pharm. Sci. 42, 365–379.
Tiwari, A.K., 2001. Modification of crystal habit and its role in dosage form performance. Drug Dev. Ind. Pharm. 27, 699–709.
U.S. Pharmacopoeia National Formulary, 1994. USP XXIII NF XVIII, 2300.
Usha, A.N., Mutalik, S., Reddy, M.S., Ranjith, A.K., Kushtagi, P., Udupa, N., 2008. Preparation and in vitro, preclinical and clinical studies of aceclofenac spherical agglomerates. Eur. J. Pharm. Biopharm. 70, 674–683.
Varlashkin, P., 2011. Approaches to quantification of amorphous content in crystalline drug substance by powder x-ray diffraction determination of crystallinity. Am. Pharm. Rev., 22–28.

Vogt, F.G., Williams, G.R., 2010. Advanced approaches to effective solid-state analysis: X-ray diffraction, vibrational spectroscopy and solid-state NMR. Am. Pharm. Rev., 58–65.

Wouters, I.M.F., Geldart, D., 1996. Characterizing semi-cohesive powders using angle of repose. Part Part Syst. Charac. 13, 254–259.

Xu, D., Redman-Furey, N., 2007. Statistical cluster analysis of pharmaceutical solvents. Int. J. Pharm. 339, 175–188.

Yadav, A.A., Yadav, D.S., Karekar, P.S., Pore, Y.V., Gajare, P., 2012. Enhanced solubility and dissolution rate of olmesartan medoxomil using crystallo-co-agglomeration technique. Der. Pharma. Sinica 3, 160–169.

Zhenhao, D., Xingxing, D., Xinyuan, S., Yanjiang, Q., 2011. Design and development of pharmaceutical excipients database. Mode. Tradit. Chin. Med. Mater. Med. 13 (4), 611–615.

Zhu, M., Ghodsi, A., 2006. Automatic dimensionality selection from the scree plot via the use of profile likelihood. Comput. Stat. Data Anal. 51, 918–930.

Zidan, A.S., Mokhtar, M., 2011. Multivariate optimization of formulation variables influencing flurbiprofen proniosomes characteristics. J. Pharm. Sci. 100, 2212–2221.